Lunds Universitets Naturgeografiska Institution

Seminarieuppsatser Nr. 55

Forest Damage, Waterflow and Digital Elevation Models

A case study of the Krkonoše National Park, Czech Republic

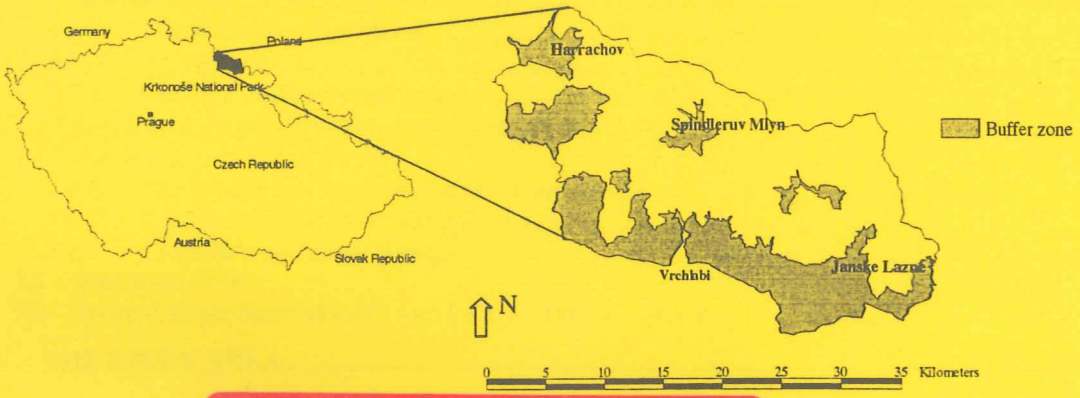

Jessica Lyborg & Lilian Thurfjell

Department of Physical Geography,
Lund University
Sölvegatan 13, S-221 00
Lund, Sweden

1999

TABLE OF CONTENTS

Abstract

In the 1970's, a widespread deterioration in forest health in Europe was observed, first for the European fir and, subsequently, also for many other tree species. Now a large portion of the forests in Europe is affected by forest decline to varying degrees.

The first aim of the study is to investigate if forest damage and forest die-back have lead to a change in waterflow. The study area is the mountain range Krkonoše National Park in northern Czech Republic. The national park is situated in a region well known as the Black Triangle, where Germany, Poland and Czech Republic meet. Acidic emissions of sulphur dioxide have caused massive deforestation of spruce mono-cultures, especially at and above the elevations of 750 m above sea level. Forest die-back till today involves a loss in forest cover of about 25%, or about 8,000 ha, of the total area.

Seven catchments in the national park were investigated regarding degree of forest damage, clear-cuts, topography, catchment size and age of forest stands. The results were then compared with changes in waterflow approximately over the period 1984-1992. The method used for investigating waterflow changes was to remove the effects of precipitation by making a ratio between data of waterflow and precipitation. In general, waterflow slightly decreased during the period whereas there was an increase in forest damage and clear-cuts. These results indicate a weak relationship between waterflow and forest changes. However, large deforestation was detected in waterflow, especially for the catchments smaller than 10 km^2.

To be able to model waterflow changes and soil erosion in the national park in the future it is of great importance to have reliable elevation maps of the area. Hence, the second aim of the study is to evaluate Digital Elevation Models (DEMs) and Digital Terrain Models (DTMs) of different resolutions (15-m and 30-m resolution maps) regarding elevation, slope and aspect in the Krkonoše National Park. The field data for the investigation was collected in the national park with GPS receiver, angle meter and compass.

Root Mean Square Error (RMSE) was calculated for the differences between field values and DEMs/DTMs. The results show that regarding elevation, the higher resolution DEM had lower RMSE values, but in slope and aspect, the lower resolution DTMs had lower RMSE. This result is probably due to that the 30-m measurements were performed in more open areas. An RMSE of approximately 3 m in elevation in both 15-m and 30-m resolution layers must be regarded as a minor error.

Acknowledgements

We would like to express our gratitude to all people working at the Department of Physical Geography in Lund for all help provided. A special thanks to our supervisor Dr. Petter Pilesjö for great support and guidance whenever needed. We would also like to thank Dr. Jonas Ardö for supplying us with a great amount of litterature.

Others of great importance to the study:

- Ing. Zdenék Fajfr and Ing. Igor Dvorak at KRNAP Administration, Czech Republic. You made this project possible by lending us equipment and by sharing your time and knowledge throughout the whole study. Thanks to you, our field trip will always be a joyful memory. We would also like to thank all others involved at KRNAP who helped us in our work.

- Dr. Ladislav Metelka at CHMI, Czech Republic who showed interest in our work and a great hospitality during our short visit in Hradec Kralove.

- Ing. Arnout ter Schure for always being positive and encouraging. Thank you for fruitful discussions and for good comments on grammar.

To friends and families, now we can start socializing again.

1. Introduction

The Krkonoše National Park (KRNAP), founded in 1963, is located in the Krkonoše Mountain range in the north-eastern part of Czech Republic. The mountains are situated in a region commonly known as the Black Triangle, where heavy air pollution from Germany, Poland and Czech Republic has been deposited during the last decades. According to Schwarz (1997), centuries of improper forest management in combination with air pollution lead to that the World Conservation Union (IUCN) in 1984 placed the Czech Krkonoše National Park among the "dirty dozen" of the most threatened protected areas in the world.

During the 15th and 16th century, the forest was devastated all over the Krkonoše Mountains when the wood was needed as energy source in industry and mining. To secure the supply of wood, the economically optimal Norway spruce *Picea abies* was planted, which yielded an unbalanced forest regarding species composition. When the air pollution drastically increased in the 1970s, the nearly monocultural forest stands were heavily damaged because of their lack in stress resistance. Other factors, such as insect calamities and extreme weather fluctuations, played a significant part as well (Bartos *et al.*, 1992).

However, as stated by Schwarz (1997), since 1991 the concentrations of sulphur compounds have decreased significantly due to reduction of the emissions from lignite-burned power plants in the Black Triangle Region. But it takes long time for forest and soils to recover from the atmospheric deposition. Therefore, it is very important that research continues in the area in order to restore the original vegetation.

A question at issue is whether the increased forest damage and clear-cuts affect waterflow in the described area. Is it true that waterflow in the water streams increases when vegetation decreases or disappears? How do size and elevation of a catchment influence the waterflow? To be able to model waterflow changes in the future, and the resulting soil erosion, it is also of great importance to have reliable elevation maps of the area. Existing elevation maps, from now on referred to as Digital Elevation Models (DEMs), are often rather different from the reality (Moore *et al.*, 1991; Hunter & Goodchild, 1997). How different are the DEMs of the national park compared to reality?

2. Aim

The aim of the project is to

1) investigate the magnitude of forest damage and clear-cuts in the different catchments in the Krkonoše National Park, and their influence on waterflow during a time period of approximately eight years from 1984 to 1992. Catchment size and elevation are also taken into consideration.
2) evaluate Digital Elevation Models and Digital Terrain Models regarding elevation, slope and aspect with resolutions of 15 m or 30 m in the Krkonoše National Park.

3. Background

This section is mainly a theoretical background of the effects of forest damage and clear-cuts on waterflow. First, the hydrological cycle will be briefly explained since it controls all water movement on earth. Second and third, different watershed and forest cover factors that affect surface runoff and erosion are discussed. Fourth, the effects of air pollution on forests, such as spruce needle loss and forest die-back, which in turn leads to clear-cutting, are taken into consideration. Fifth, the effects of forest re-establishment on surface runoff and the arising difficulties are presented. Finally, a brief description of Digital Elevation Models and Digital Terrain Models ends the chapter.

3.1 The hydrological cycle

The earth's water is in constant motion in a closed system called the hydrological cycle. It moves continuously from the atmosphere to land, plants, freshwater bodies and oceans (storages) and then back into the atmosphere. The main components of the cycle are evapotranspiration, precipitation, infiltration, percolation, groundwater interflow and runoff. A general assumption is that water can not disappear. Precipitation falling within a catchment is distributed between evapotranspiration (ET), runoff (R) and storage change (ΔS). This relationship is expressed in the mass balance equation (Grip & Rodhe, 1994):

$$P = ET + R + \Delta S \qquad \text{(Eq. 1)}$$

3.1.1 Evapotranspiration

Evapotranspiration is the process that returns the water to the atmosphere. It can be divided into two sub-processes: evaporation and transpiration. Evaporation is the transfer of moisture from open surface-water bodies as oceans, lakes, reservoirs, or from vegetation and ground surfaces, to the atmosphere. Transpiration involves the removal of water from soil by the osmotic pressure of vegetation root system, transport of the water into the leaf and evaporation of the water from the leaf interior into the atmosphere (Ward & Elliot, 1995).

3.1.2 Precipitation

The evapotranspirated water is stored as water vapour in the atmosphere where it together with small water droplets can condense on airborne particles and form clouds. The particles enter the atmosphere through dust, volcanoes, industrial exhaust, forest fires, ocean salt etc. (Ward & Elliot, 1995). When a cloud cools and the amount of condensed water increases, droplets can grow bigger and reach a size that causes them to fall to the ground as water droplets or, if the temperature is well below freezing, as ice crystals. Snow and ice can then be stored for very long periods (Ahrens, 1994).

3.1.3 Infiltration and percolation

Infiltration is a process by which water enters a soil in a downward direction from the surface via pores or small openings. Percolation is the flow of water through the soil or porous substance. The downward movement is due to tension and gravitational forces in the soil matrix. The infiltration rate depends on the physical characteristics of the soil, the moisture of the soil, the type and extent of a vegetation cover, the slope of the surface and the nature of the rainfall. Water infiltration into the ground decreases surface runoff, soil erosion and the movement of sediments and pollutants into water systems (Grip & Rodhe, 1994; Ward & Elliot, 1995).

3.1.4 Groundwater interflow

Deep percolation is mainly beyond the reach of plant roots, thus this water contributes to replenishing the groundwater supply. As water percolates, some of it may reach a layer of impermeable soil, such as clay, or rock, which restricts water from moving downward. The water starts moving laterally along this layer as interflow and eventually discharges to a stream or lake (Grip & Rodhe, 1994; Ward & Elliot, 1995).

3.1.5 Surface runoff

Surface runoff exists when the rate of water application to the ground exceeds the rate of infiltration into the soil. This is the surface-water contribution to a stream. Once surface runoff has started, the water continues to flow until it reaches a stream, river or an area of permeable soil or rock. The terms watershed and catchment are used to delineate areas of different sizes, which contribute runoff at their outlets. A watershed boundary may consist of natural topographic features and the boundary is often called the watershed divide because it divides the direction of the flow. Surface flow will never occur across a boundary and all flow within it will drain to the watershed outlet (Grip & Rodhe, 1994).

3.2 Watershed factors affecting runoff

Besides precipitation, watershed factors that effect runoff are e.g. size, shape, topography, geology, soil and vegetation.

3.2.1 Catchment size and shape

Catchment size influences runoff in a number of ways. In general, total runoff per unit area increases with catchment size as a result of the increasing baseflow, even though the effect is very variable. It is also of general knowledge that small catchments respond quicker and differently to hydrological variations than large catchments do. Among others, Pilgrim *et al.* (1982) showed that compared to small watersheds, changes are often not reflected on large catchments where the proportion of the area affected is relatively small. For instance, a small watershed can be heavily affected by land cover changes, road constructions and urbanisation.

Circular or fan-shaped watersheds have high rates of runoff when compared to for instance long narrow watersheds. This is because runoff from different points in the circular watershed is more likely to reach the outlet at similar times. For the narrow watershed, tributaries join the main stream at intervals along its length. Hence, peak flow at the gauge is less but persists for a longer time (Ward & Elliot, 1995).

3.2.2 Topography

Topography has an influence on the velocity of waterflow on land surfaces and in channels. Runoff will occur in the direction of the slope and perpendicular to the contours in a topographic map. Slopes get different rates of solar radiation depending on the aspect of the slope. This will affect temperature, soil water content and vegetation, and it is also important for soil freezing (Ward & Elliot, 1995).

Steep land is more vulnerable to water erosion than flat land for the reason that erosive forces, such as splash, scour and transport, have a greater effect on steep slopes. When the soil cover is weathered, large trees will have difficulties remaining erect and the nutrient uptake begins to suffer. The trees become more sensitive to stress situations, e.g. insect attacks, frost damage and air pollution. Long slopes also yield greater erosion rates. Slope length is measured from the

point where the surface flow originates (usually the top of the ridge) to the outlet channel or a point downslope where deposition begins (Hudson, 1981). The shape of a slope (Figure 1) also affects soil loss (Young & Mutchler, 1969, in Hudson, 1981). For instance, a uniform slope loses more soil than a concave slope, but less than a convex slope.

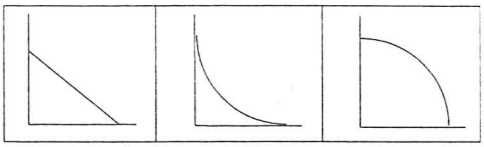

Figure 1. *Uniform (left), concave (centre) and convex slope (right).*

3.2.3 Geology, soil and vegetation

Weathering and erosion play a significant role in the formation of soil and physical characteristics of a watershed. Geology has for instance established the surface and subsurface flow systems. Geological features such as rock formations, faults etc. and processes have also helped define ridges and divides between the watersheds (Moldan & Cerny, 1994).

The resistance of a soil to erosion depends on many factors. Hudson (1981) described erosivity as the potential ability of rain to cause erosion. It is a function of the physical characteristics of precipitation, e.g. drop size, intensity and length of precipitation, and can therefore not be modified by man. Erodibility is the vulnerability or susceptibility of the soil to erosion. It is a function of both the physical characteristics of the soil and the management of the soil. For example, sandy soils are more easily eroded than hard clay and some crops protect the soil better than others do.

Presence of organic matter, stronger subsoil structure and greater permeability generally decrease erodibility. In general, soils with high silt contents tend to be the most erodible. However, as discussed by Wischmeier & Smith (1978), a soil with a relatively low erodibility factor may show signs of serious erosion when it occurs on long or steep slopes or in localities with numerous high-intensity rainstorms. On the other hand, a soil with a high natural erodibility factor may show little evidence of actual erosion under gentle rainfall when it occurs on short and gentle slopes, or when the best possible management is used.

Vegetation cover protects the surface from raindrop impact and reduces the amount of water available for runoff by consuming it and by improving the infiltration capacity. The cover also increases surface roughness, which decreases the velocity of runoff. In addition, plant roots help to keep the soil in place. Aspects of vegetation controlling surface runoff include canopy density, height, degree of cover, root density, mulch and water consumption. For example, a grass cover is generally the most efficient defence against soil erosion by running water (Cooke & Doornkamp, 1990).

3.3 Influence of forest cover on runoff and erosion

Rain falling on a forest canopy will adhere to the leaves and branches, a process called interception, and some part of the precipitation will evaporate back to the atmosphere. As rainfall continues, water will fall off and drip onto lower leaves and branches until the interception capacity of the tree is nearly full. At that point, some of the water will fall through to the ground as throughfall and some will flow down the trunks and stems as stemflow (Ward & Elliot, 1995).

Interception and stemflow rates are controlled by a variety of factors where the most important one is the type of tree. In general, coniferous trees have a larger interception capacity compared to deciduous trees. In some coniferous stands, 20-40% of the total precipitation is evaporated from the interception storage back into the atmosphere (Materna). Snowfall interception is more a function of branch strength and canopy strength. The magnitude of snowfall interception capacity is generally greater than that of rainfall (Ward & Elliot, 1995).

Soil erosion in forests is usually less severe than the erosion from arable land. A mass of fine roots and decaying leaves form a mat of organic matter at the soil surface. The layer is resistant to movement from raindrop impact and protects the underlying mineral particles from moving. Vegetation canopy in combination with the accumulation of forest litter often gives a complete protection of the soil surface. The cover yields a lower rate of erosion and reduced peak floods compared to similar land under other uses. However, as discussed by Hudson (1981), even if a rainfall is of fairly low intensity erosion may arise under a tree canopy. Rain reaches the canopy and eventually drips through, but the size of the drops that slowly drip from the leaves is greater than the natural raindrops. The result is that tree cover does not automatically provide protection against floods and erosion.

The large canopy system above ground is mirrored by an equally large root system beneath the ground. These roots create a network of large pores through which water can flow much faster than in the soil matrix itself. The large leaf area and this root access to deeper water allow for greater transpiration rates (Ward & Elliot, 1995).

3.4 Air pollution and forests

Physiological stress on trees promoted by air pollution brings about a higher sensitivity to high winds, snow, pests and root decay. A consequence of air pollution is the reduction in biomass of leaves and needles. Spruce in a healthy state has 7 to 9 year sets of needles while a damaged tree has only between one and three of the youngest sets left. Hence, as stated by Kubíková (1991), interception is lowered, resulting in an increased water quantity falling to the ground.

3.4.1 The influence of air pollution on spruce needles

The surface of spruce needles in a healthy state has a dense layer of wax crystals, which protects the needles against dehydration and parasite attacks. According to Ulfvens (1989), the effects of pollution on needles can be divided into three phases:

1. The dense wax layer first starts to decompose and the wax crystals form lumps on the needle surface. Water and nutritive substances leak where the protective wax layer is missing and stomata may be clogged.
2. The needle begins to produce stress enzymes, which can to some extent neutralize the pollutant in the needle. This process, however, takes a lot of energy and results in a negatively affected growth. Thus, the needles become smaller and shorter.
3. Finally, the needle has lost most of its resistance and vitality. The disturbance in photosynthesis leads to an increase of sugar content and this in turn attracts insects and plant lice, which completely destroys the needle.

Ulfvens (1989) also stated that the normal approach in Europe is to divide the trees into five damage classes regarding how much of the needle mass is estimated to be lost in the tree crown. The least affected class has a needle loss of 11-25% whereas the most affected includes completely dead trees only.

3.4.2 Topography and forest damage

The growth of a forest stand and its resistance to stress is mainly controlled by topography. Elevated areas have lower mean temperatures, shorter vegetation periods and larger amount of precipitation compared to lower areas. Thus, it demands a vegetation type that is tolerant to tough climate. Dwarf pine and dwarf birch are examples of this type of vegetation (Dollard *et al.*, 1983). The major disadvantage with Norway spruce is its sensitivity to the harmful effects of sulphur dioxide. The more so, if the effects are accompanied by weather extremes (Grossinho, 1996). Norway spruce is therefore extremely sensitive to air pollution under the ecological conditions prevailing at high altitudes (Materna).

Dollard *et al.* (1983) noted that interception of fog, mist, rime and cloud is often large at high altitudes. This yields a large wet acidic deposition, sometimes up to ten times higher than rain and is thereby potentially a contributing factor in forest decline. The aspect of a slope is another factor playing a significant role in forest damage. A stand that is located on a slope with the aspect towards a pollution source is more affected than a slope on the lee-side (Ling, 1995).

According to a study in Krusne Hory in north-western Czech Republic, Ardö *et al.* (1997) reached the conclusion that forests in elevations above 1,000 m are very exposed to air pollution, due to harsher climate conditions and shorter vegetation periods. They also have a very low growth rate compared to forests at lower elevations. The largest spruce forest stands were located between 400 and 1,000-m elevations where the climate was most suitable. Between 800 and 1,000 m an increasing trend in yearly needle loss and forest death was present, while there was more of an even and continuous needle loss between elevations of 600 and 800 m. The same conclusions have been reached by several other researchers, such as Nelleman & Frogner (1994).

3.4.3 Clear-cuts and forest damage

A change in vegetation type and forest damage influences both surface runoff and ground water storage. Clearing of for instance damaged forest will remove the network of roots beneath the ground and the organic mat on the surface, yielding a rise in groundwater table and increased surface runoff (Pilgrim *et al.*, 1982). The high groundwater table enables the surface runoff to respond quicker to precipitation, resulting in increased runoff peaks in the waterflow compared to when the water table is low and infiltration capacity is higher (Grip & Rodhe, 1994). Furthermore, the transpiration surface storage decrease when removing the forest, which also contributes to increased surface runoff.

An investigation of impacts of forest treatments on water yield by Hornbeck *et al.* (1993) showed that initial increases in water yield occurred directly after forest cutting and diminished usually within 3-10 years. However, Pilgrim *et al.* 1982), stated that the increase in runoff volumes and flood peaks with clearing are so highly variable that no general relationship can be established.

According to Materna the increasing water quantity will not always increase the runoff from the watersheds. The development of resistant grasses and other plant species are often improved and these plants have an important influence of the water management in the stand. Materna also noticed distinct differences in the runoff during the year between damaged and healthy forest

stands. The disturbance of crown closure of spruce stands under the influence of air pollution, decreases the protection of snow resources in the mountains in spring and causes the snow to thaw more rapidly.

3.5 Reforestation

When re-establishing the forest in a clear-cut area the evapotranspiration increases, the groundwater table drops and the surface run-off returns to its original state. However, the higher groundwater table, caused by the clear-cuts, complicates the forest regeneration in valleys and flat areas. The roots of the young plants can not transpire due to excess water content in the ground and the growth will deteriorate (Grip & Rodhe, 1994).

Another problem with reforestation of clear-cuts is that the soil can be poor in nutrients. When clear-cutting, the soil receives large amounts of waste material, such as branches and needles, which is decomposed and a lot of nutrients are released. Before grass and other vegetation have been established in the clear-cut, there are very few living roots that can assimilate these released nutrients and hence they will be washed out into waterflows and groundwater, yielding a soil poor in nutrients (Grip & Rodhe, 1994).

3.6 Digital Elevation Models and Digital Terrain Models

In recent years, there has been an increase in the use of a digital system called Geographic Information System (GIS). It is being used to map, model, visualise, and analyse complex data sets and it is now routine to create digital databases of for instance ground elevation, soil class, land cover class and ownership. The data can then be used as input in a model. Finally, the results of processing are outputs that can be used as a basis for decisions. However, these spatial databases are often of low quality since many are derived from printed maps which in turn are the result of subjective interpretation of the landscape (Moore *et al.*, 1991; Hunter & Goodchild, 1997). It is therefore important for users to know the quality of the products to know if it is accurate enough to suit their purposes.

According to Skidmore (1989), DEMs are digital representations of terrain surfaces, for instance a quadratic grid of elevation points for which the x (northing), y (easting) and z (elevation) are recorded in the centre of the cell. Often the grid values are sampled irregularly and then interpolated to a grid. The process will include a number of errors. For instance, when using photogrammetry for producing elevation points from an aerial photography, operators tend to underestimate elevation when moving uphill and overestimate it when moving downhill (Hunter & Goodchild, 1997).

Slope and aspect can be derived from DEMs in a number of ways. These calculated layers are called Digital Terrain Models (DTMs). Slope is the maximum rate of change in altitude and aspect is the compass direction of this maximum change (Skidmore, 1989). Besides slope and aspect, other important variables e.g. slope length, size and shape of drainage basins can be calculated from a DEM. These important parameters are often required in soil erosion modelling, hydrological applications, ecological models and management of natural resources (Pilesjö, 1992).

4. The Study Area

In 1963, the former Czechoslovak government declared Krkonoše Mountains (Giant Mountains) the first Czech National Park (Figure 2). The area of the Czech biosphere reserve is 54,787 hectares of which 36,358 hectares are the national park and 18,430 hectares are the buffer zone. The main reason to establish the national park was to preserve the unique habitat for the future, but there were other reasons as well. Since Labe (Elbe) River originates in the Krkonoše Mountains, the Czech government wanted to maintain good water quality. It was also of importance to protect the area since it is the northern-most range in Central Europe with well developed sub-alpine and alpine zones. The region also needed protection against the rapid development of tourism and recreation, which legislation would control (Brewer, 1993).

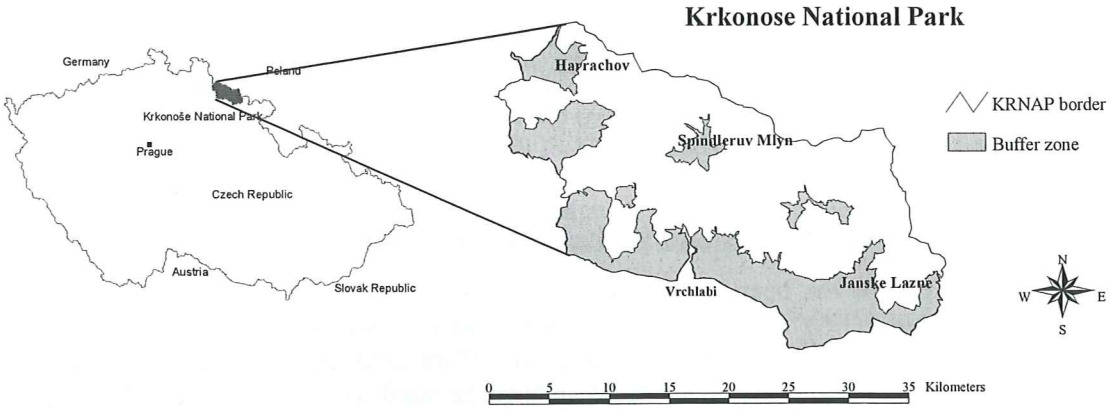

Figure 2. *Overview of the study area. The map is based on digital layers collected at KRNAP.*

4.1 Location and topography

Krkonoše Mountains (Figure 3) belong to a ridge stretching along the Czech/Polish border and they are located in the Bohemian massif, which also takes up the adjacent regions of Moravia, Poland and Germany. The Krkonoše are divided into two parallel ridges, which are linked by the high upland plateaux in the west Sudeten system. The outer ridge forms the border between Czech Republic and Poland, while the inner Czech ridge is lower than the outer one and divided by the Labe River. It is also narrower with steep slopes and several traces of glaciers (Grossinho, 1996).

The mountain range is about 39 km long (east to west) and between 5 and 15 km wide (north to south) and it is the highest range in Czech Republic. Its maximum elevation corresponds to the peak Snézka with a height of 1,602 m whereas the lowest point is located about 450 m above sea level (Dunda, 1991).

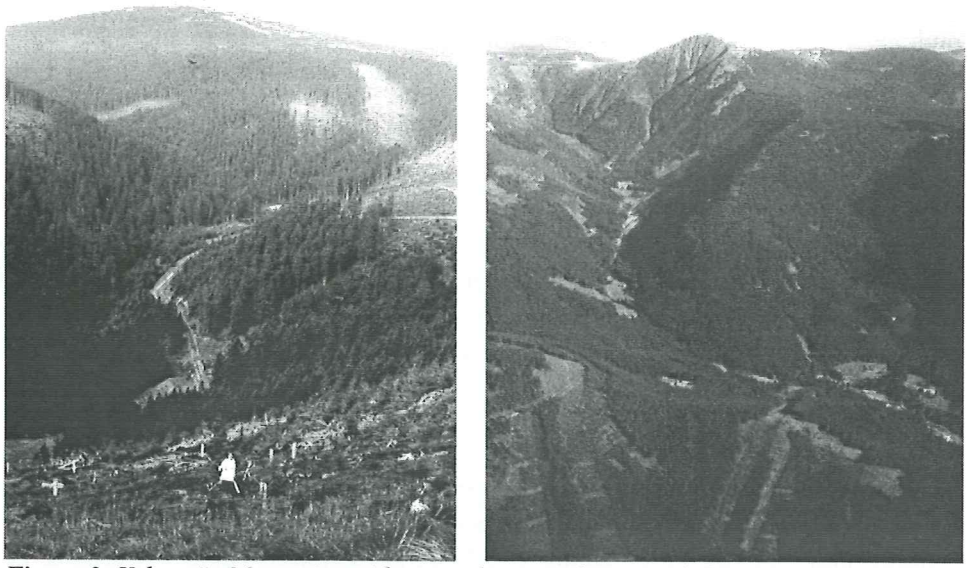

Figure 3. *Krkonoše Mountains with steep slopes and traces of glaciers. Snézka, the highest peak in Czech Republic, is viewed in the right photograph.*

4.2 Geology and geomorphology

Krkonoše Mountains consist of a small granitic core, surrounded by a broad belt of metamorphic rock. In Late Tertiary, the pressure of the Alps and Carpathian Mountains tectonically ruptured the Bohemian massif. Most of the Czech mountains were then slowly uplifted to their present height. Great valley erosion occurred, forming rivers from north to south on the Czech side. The deepening of the valleys made the individual ridges and peaks more distinct and the whole mountain range became more dissected (Korenská, 1990).

During the Ice Age, in Quaternary, the valleys were widened and deepened and became more U-shaped. The ice also gave rise to morain deposits and water falls of which Pancavský vodopád is the highest one in the Czech Republic (148 m). After the Ice Age, the climate became similar to that of today and the proceeding water erosion developed ravines, which still is an ongoing process on the steep slopes. In the study of Korenská (1990) it was observed that debris avalanches are the most dominant slope processes in the region today. Rock slides, rock falls, solifluction and an intensified number of avalanches, due to deforestation, are other recent processes worth mentioning.

4.3 Climate

The Krkonoše Mountains are located in the temperate climatic zone where prevailing western winds bring in wet air from the Atlantic Ocean. This air circulation pattern yields low temperatures with long and cold winters, short summers, abundant precipitation and frequent strong winds. Mean annual temperature varies between 0°C and +6°C, depending on altitude and exposition, and temperature inversions are a common phenomenon. Krkonoše Mountains have a precipitation of 1200 to 1600 mm on the peaks and around 800 mm on the foothills (Cerny & Paces, 1995; Grossinho, 1996).

4.4 Vegetation

The biogeographical location of the Krkonoše Mountains has given rise to the most valuable ecosystems. As stated by Schwarz (1997), alpine tundra, subarctic peat bogs, glacial cirques, dwarf pine stands, original spruce stands and mixed forests are just some of the ecosystems present in the area. Many of the plants are endemic where, for example, glacial cirques host several subalpine and alpine species, communities and ecosystems (Dunda, 1991).

Approximately 87% of the forests in the Krkonoše Mountains consist of Norway spruce (*Picea abies*). The second most common species is the mountain pine (*Pinus mugo*) with 6.1%. Other species are beech (*Fagus sylvatica*), birch (*Betula sp.*) and maple (*Acer sp.*) which only account for a small percentage. The original forest cover was composed by a well-balanced mixed forest of coniferous and deciduous trees. However, it is more cost-efficient to transform a mixed forest into an even-aged stand (Cerny & Paces, 1995; Grossinho, 1996).

Plant growth is mainly influenced by altitude, air temperature and changes in length of vegetation period, i.e. the number of days with a mean temperature higher than 5°C. This divides the Krkonoše Mountains into four vegetation zones, which are presented in Table 1 (Cerny & Paces, 1995; Grossinho, 1996).

Table 1. Vegetation zones in the Krkonoše Mountains (Grossinho, 1996)

Vegetation zone	Altitude (m)	Vegetation cover
Sub-montane	400-800	Mixed forests
Montane	800-1250	Norway spruce forests
Sub-alpine	1250-1450	Swiss mountain pine and meadows
Alpine	1450-1602	Debris, alpine tundra with herbs, mosses and lichens

The sub-montane zone covers the foothills and the lower regions of the Krkonoše. Originally, there was only deciduous forest in this zone. However, today it has been replaced with Norway spruce or meadows in most areas except on less accessible slopes. The montane belt is also dominated by planted Norway spruce, but it is in a fairly poor health condition caused by frost events, blow down, breakage in tops, rot and insect calamities (Korenská, 1990). The Swiss mountain pine, *Pinus mugo*, dominates the sub-alpine zone whereas the timberline is reached in the alpine zone (Korenská, 1990).

At the turn of 1978/1979, an unusual frost event occurred in the Krkonoše Mountains, where the temperatures fell dramatically about 20°C within ten hours. This event was followed by several days of frosty weather with very low temperatures. Such a frost shock episode provoked very severe damage in various Norway spruce stands of all age classes (Grossinho, 1996).

4.5 Management and future plans

Forest management in the Krkonoše Mountains is based on site conditions, information about the emission load and knowledge on how the ecosystem responds to an emission load. It is of great importance to preserve the existing ecosystems, species and biodiversity, which is achieved by natural regeneration, reforestation etc. A primary goal is to reduce the spruce population and alter it with deciduous trees or fir (Schwarz, 1997). The alteration gives better soil properties since spruce needle litter leads to acidification of the soil (Gebas *et al.*, 1998).

According to Schwarz (1997), the area has been divided into zones depending on their natural values (Figure 4):

- Zone I (4,152 ha) covers areas with the most significant nature values. These are ecosystems that have been altered very little by man. There is no timber logging in this zone which leads to a financial loss.
- In zone II (3,046 ha) the stands affected only slightly by emissions are preserved whereas damaged stands are regenerated to bring the ecosystems closer to their natural state.
- Zone III and the buffer zone (approximately 28,000 ha and 18,400 ha, respectively) include ecosystems which have been considerably altered by man. The aim of conservation in these two zones is to prevent any further negative influence on the national park. The towns within the park (Harrachov, Rokytnice, Spindleruv Mlyn and Pec pod Snezkou) are located in the buffer zone.

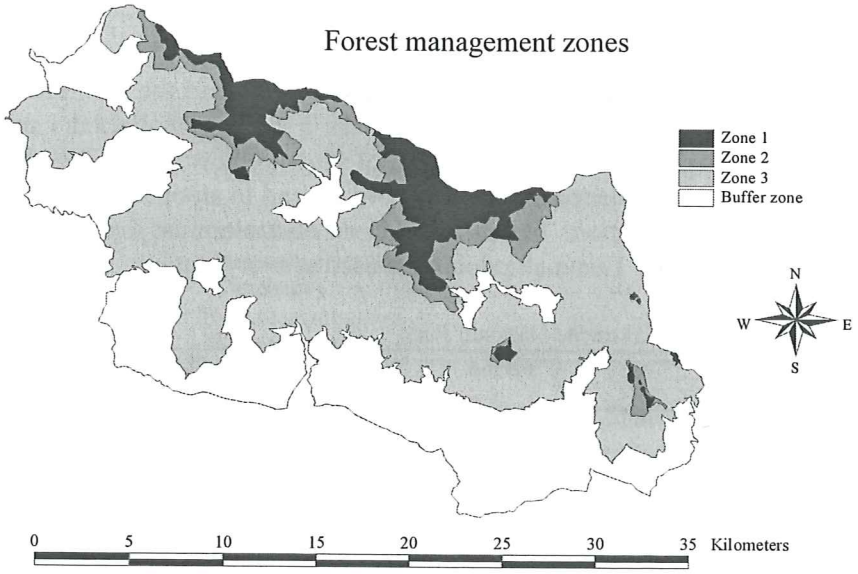

Figure 4. *Forest management zones in Krkonoše National Park. The map is based on digital layers collected at KRNAP*

Within the last fifteen years, approximately 8,000 hectares or about 25% of the forest in the national park have totally disintegrated and an additional 8,000 hectares of forest ecosystems are potentially endangered. This forest die-back has yielded and still yields a reduction of the CO_2 fixation. The Dutch foundation Forests Absorbing Carbondioxide Emission (FACE) has the objective to increase the forested areas in the world to regain larger CO_2 fixation. Hence, the FACE foundation funds the necessary research to restore semi-natural forest ecosystems in the national park (Gebas *et al.*, 1998).

5. Material and Methods

Data collection, methods for the production of digital data and fieldwork in Czech Republic are presented first in the chapter. Thereafter, methods for data analysis are discussed.

5.1 Data collection

Data used in the study were collected in Czech Republic. Precipitation and waterflow data (monthly average) were collected at the Czech HydroMeteorological Institute (CHMI) in Hradec Kralove whereas all digital layers were collected at KRNAP Administration situated in Vrchlabi. The coordinate system of the digital maps is Krovak, which is the Czech national grid. Beside these data, a field investigation in the Krkonoše National Park was carried out during September 1998 where elevation, slope and aspect were measured.

5.1.1 Digital data for the study of waterflow changes

Precipitation is measured every day at 07.00 AM in three stations (Table 2) in the national park. The gauge has an area of 500 cm^2 at the top and is funnel-shaped to lead the precipitation into a box below. The funnel is removed during the winter to make it easier to collect the snow in the box but on the other hand it is possible for some amount of snow to blow away. The snow is then melted and measured. The gauge is placed one meter above ground in an open area to remove the effect of for instance forest interception. The distance to an obstacle must therefore be at least ten times the height of the obstacle. This methodology is used at every station.

Table 2. Precipitation stations in the Krkonoše National Park

Station	Period	Height above sea level (m)
Spindleruv Mlyn – Svaty Petr	1977-1994	852
Dolni Dvur – Rudolfov	1963-Sep1998	600
Horni Marsov	1961-Sep1998	606

The water level in a watercourse is measured either manually, by reading off a measuring stick in the waterflow, or automatically, with a sensor connected to a logger, at 7.00 AM in seven stations (Table 3). The water level is then transformed into waterflow with some calculations. The catchments used in this study vary from 6 to 82 km^2 in size, which according to Jenkins *et al.* (1994) are regarded as small catchments. However, the catchments Spindleruv Mlyn, Labska and Horni Marsov will be referred to as large catchments, since they are so much larger than the other four.

Table 3. Surface waterflow stations in the Krkonoše National Park.

Station	Period	Catchment area (km^2)	Height above sea level (m)
Spindleruv Mlyn	1920-1926, 1989-1997	53	714
Labska	1907-1926,1987-1997	61	663
Cerny Dul	1982-1997	7	766
Modry Dul	1965-1997	3	1026
Obri Dul	1988-1997	9	900
Horni Mala Upa	1989-1997	6	912
Horni Marsov	1931-1940, 1949-1997	82	570

Three digital vegetation maps and three forest damage maps from 1984, 1990 and 1992 were used to investigate land cover changes. These maps were classified and digitized by Ing. Martin Vyklický at former Czech Institute for Nature Protection, Prague, in 1992-1993. The classifications are based on satellite imagery, where bands 3, 4, 5 and 7 in Landsat TM4 (1984) and TM5 (1990 and 1992) were used. The software for the classification was performed with EASI/PACE.

First, a forest/non-forest mask was produced, using unsupervised clustering. Forestry maps and air photos were used to aggregate and correct the classes to produce the mask. Second, the forest was classified using Gaussian Maximum Likelihood supervised classification (MLC), resulting in eleven vegetation classes (Table 4). Training sites were selected by means of air photos, forestry maps and forestry management plan database. Their consistency was checked, where possible, in field.

Table 4. Description of the classes in the vegetation maps from 1984, 1990 and 1992.

Class	Description
1	Water
2	Spruce stands up to ten years
3	Spruce stands more than ten years
4	Mountain beech stands
5	Deciduous stands
6	Mixed stands
7	Mixed spruce and mountain pine
8	Mountain pine stands
9	Clear-cuts
10	Mountain meadows
11	Alpine grasslands

Finally, the separation of five forest damage classes (Table 5) was made manually using air photos, based alone on the spruce category. The separated areas were classified by a second MLC.

Table 5. Description of the five spruce damage classes from 1984, 1990 and 1992.

Class	Description
1	Healthy
2	Light
3	Moderate
4	Strong
5	Very strong

An accuracy assessment of the vegetation maps for each year was evaluated to determine the reliability of using Landsat TM data for actual vegetation cover mapping. The Kappa coefficient was high for all years (1984: K = 0.959, 1990: K = 0.974 and 1992: K = 0.928) (van der Horst *et al.*, 1995). The Kappa coefficient is a measure of association and can be calculated when two images have exactly the same number of categories. It ranges from 0.0 indicating no correlation to 1.0 indicating perfect correlation. The spruce damage maps were not evaluated.

A layer showing the age of forest stands with 24 classes divided into intervals of ten years, from 1 to 235 years, was made by the Institute of Forest Ecosystem Research (IFER) in Czech Republic during 1998 and presents the forest status in 1992. The deforestation between 1979 and 1995 is presented in a map with eight classes (Table 6). The map was produced by Martin Síma in 1995. These two layers (forest age map and deforestation map) have not been evaluated.

Table 6. Categories in the map representing deforestation between 1979 and 1995.

Class	Description
1	Forest-free area 790531
2	Forest 950710
3	Deforested in: 790531-820601
4	Deforested in: 820601-840711
5	Deforested in: 840411-860615
6	Deforested in: 860615-900829
7	Deforested in: 900829-920919
8	Deforested in: 920919-950710

5.1.2 Digital data for investigation of DEMs/DTMs

Two DEMs of the Krkonoše National Park with 15 and 30 m resolution were used in the study. The DEMs are interpolated from a contour line layer with the equidistance of 25 m, which was digitized in 1993 from paper maps. The scale of the paper maps is 1:10,000 and has an equidistance of 5 m. The original paper maps were produced manually by measuring in field in 1979 and then updated in 1990.

Slope and aspect were derived with Arc/Info GRID's algorithm from the DEMs (15 and 30m). The algorithm was created by Horn (1981) and is a third-order finit difference method (Skidmore, 1989). It uses eight grid points to calculate each slope and aspect value with unequal weighting coefficients for the nearer elevation values (Jones, 1998). According to Skidmore (1989) the algorithm can be written as:

$$[\delta z/\delta x]_{i,j} = \left[\left(z_{i+1,j+1}\right)+2\left(z_{i,j+1}\right)+\left(z_{i-1,j+1}\right)\right]-\left[\left(z_{i+1,j-1}\right)+2\left(z_{i,j-1}\right)+\left(z_{i-1,j-1}\right)\right]/8\Delta X \qquad \text{Eq.2}$$

and

$$[\delta z/\delta y]_{i,j} = \left[\left(z_{i+1,j+1}\right)+2\left(z_{i+1,j}\right)+\left(z_{i+1,j-1}\right)\right]-\left[\left(z_{i-1,j+1}\right)+2\left(z_{i-1,j}\right)+\left(z_{i-1,j-1}\right)\right]/8\Delta Y \qquad \text{Eq.3}$$

where
$z_{i,j}$ = centre cell of the window located at the *i*th row and *j*th column
ΔX = spacing between points in the horizontal direction
ΔY = spacing between points in the vertical direction

Slope (G) is then defined as

$$\tan G = \sqrt{(\delta z/\delta x)^2 + (\delta z/\delta y)^2} \qquad \text{Eq. 4}$$

while aspect (A) is defined as

$$\tan A = \frac{(\delta z/\delta x)}{(\delta z/\delta y)} \qquad \text{Eq. 5}$$

Skidmore (1989) and Jones (1998) have compared this method with a number of other methods for calculating slope and aspect. Both authors have come to the conclusion that Horn's algorithm is one of the better methods.

5.1.3 Field data collection

Elevation, gradient and aspect were measured in field to evaluate the DEMs and DTMs of Krkonoše National Park. The positioning (x, y) and elevation (z) of the sampling point was collected with a GPS receiver, whereas gradient and aspect were measured manually. To obtain at least a hundred sampling points road sampling (Pilesjö, 1992) was used. For this purpose, the national park was divided into 13 areas of about 25 km^2 each of which roads marked as accessible in the map legend were numbered. Since the largest roads often are stretched in valleys, only the smaller roads (accessible by car) were chosen.

The roads in each area were randomized in Excel to avoid bias effect (human influence of the result). The sampling was then performed along the roads in this order where a passenger car could come through. Once in field, many roads turned out to be suitable only for terrain cars and had to be excluded from the order. Elevation, gradient and aspect were then measured in eight points in each of the 13 areas at a 400-meter interval (Figure 5).

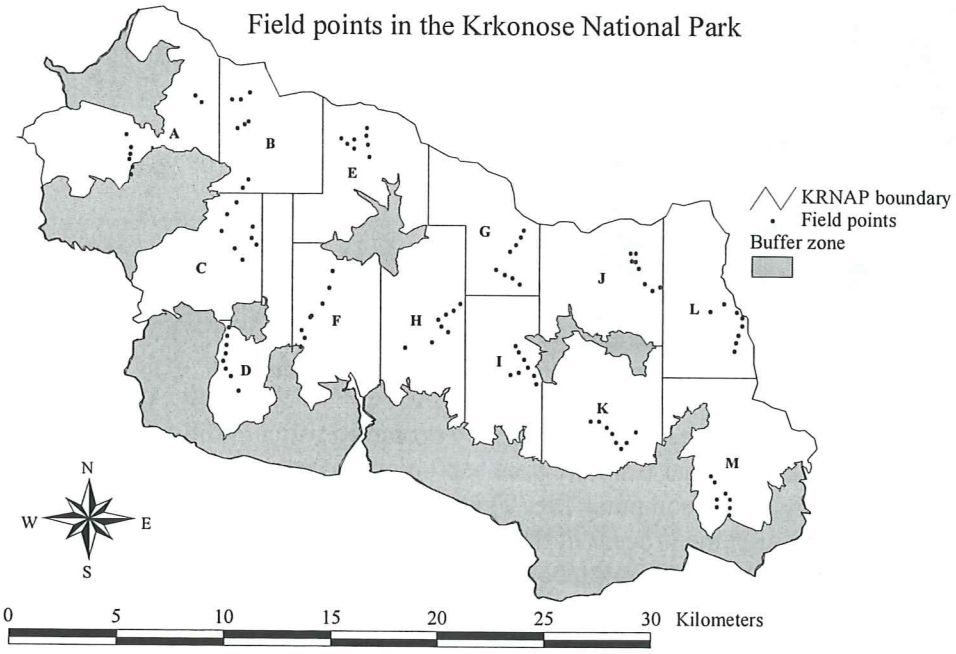

Figure 5. *Krkonoše National Park divided into thirteen areas (A-M) with eight sample points in each, collected by road sampling. The map is based on digital layers collected at KRNAP*

5.1.3.1 Elevation

Elevation was measured with a Trimble PathFinder ProXR GPS receiver. According to Trimble (1995) the receiver has a position accuracy in the lower half of the sub-meter range with initial accuracy at 50 cm to 75 cm. The GPS receives a position from the available satellites every second. After differential correction, an average is calculated of the positions received at the same point. An evaluation of the accuracy of the used GPS receiver was performed by using the results from measuring at five known geodetic points. To investigate how many positions are needed to yield the optimal accuracy of the GPS readings, 450 and 900 positions were measured at each geodetic point.

The GPS antenna was attached to a tripod to receive signals from exactly the same point during the entire measurement (Figure 6). The height of the antenna was then measured and added into the logger file to adjust the height in the output file. At each of the 104 sampling points (Figure 5) the GPS received about 900 positions with a Position Dilution of Precision (PDOP) mask of six in 3D mode. PDOP is a measure of the current satellite geometry. The lower the PDOP value, the more accurate the GPS positions. A PDOP of four and below gives excellent positions, between five and eight is acceptable and a value above nine is poor (Trimble, 1995).

Figure 6. *The Trimble GPS receiver and antenna to the left in the photograph.*

After returning from field, data was differentially corrected using PathFinder software. This was performed by downloading data from the base station in Prague, which had recorded the error for each satellite directly into a computer file. The rover (the used GPS receiver) file and the base file were then run through the process in the software. The 900 position readings from each point were corrected and averages of longitude (x), latitude (y) and elevation (z) were calculated.

5.1.3.2 Gradient and aspect

Gradient was measured with the angle indicator INOGON® 90, which has an accuracy of 0.2°. The indicator was fixed to an aluminum profile, which in turn was placed with magnets on an iron plate fastened to a tripod (Figure 7). The iron plate could be inclined and moved vertically to the desired position and then locked. Two stretchable cords, 15-m and 30-m, were stretched (one at a time) between two iron poles in the aspect direction with the centre located as close as possible to the GPS receiver. These lengths of the cords were chosen since the resolution of the DEMs/DTMs are 15-m and 30-m. The aluminum profile was then inclined to fit the cord and the angle was measured (Figure 7). Gradient and aspect were measured at the same sampling 104 points as the elevation with the 15-m cord. However, since it was difficult to stretch the 30-m cord in dense forest, gradient and aspect were only measured at 45 points with this cord.

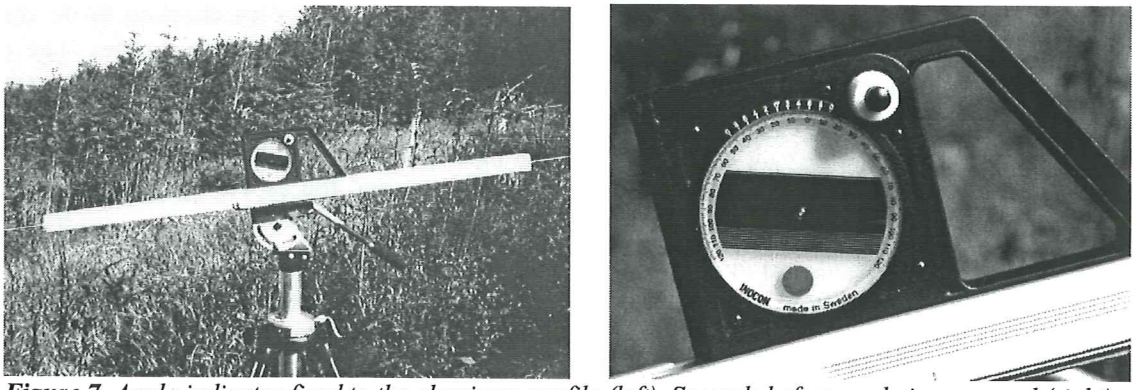

Figure 7. *Angle indicator fixed to the aluminum profile (left). Seconds before angle is measured (right).*

To keep the error of the gradient measurements low, for instance below 0.2° (which is the accuracy of the angle indicator) the maximum vertical and horizontal movements of the cord and poles, respectively, were calculated. If the cord is not fastened at the same height on the two poles, the angle of the slope will not be correct. To keep the error below 0.2°, the height between the poles can only differ a certain amount. This margin of error was calculated for both 30-m and 15-m measurements with the angle ratio for tangens (Figure 8). The results were that the cord could differ 10 cm in height for the 30-m cord and only 5 cm for the 15-m cord, assuming the poles to be vertical.

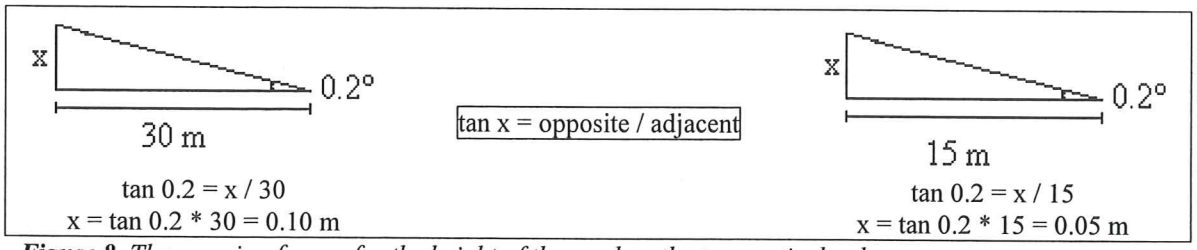

Figure 8. *The margin of error for the height of the cord on the two vertical poles.*

If one of the two poles is not exactly vertical, the height of the cord will differ from one side to another. To keep the cord within 10 and 5-cm difference (which keeps the error below 0.2°), one of the poles can incline some degrees for the 30 and 15-m measurement, respectively. This error was calculated for both measurements with the angle ratio for cosine (Figure 9). The margin of error for the vertical angle was 25° for the 30-m cord and 18° for the 15-m cord, assuming that the cord was fastened at the same height on the two poles.

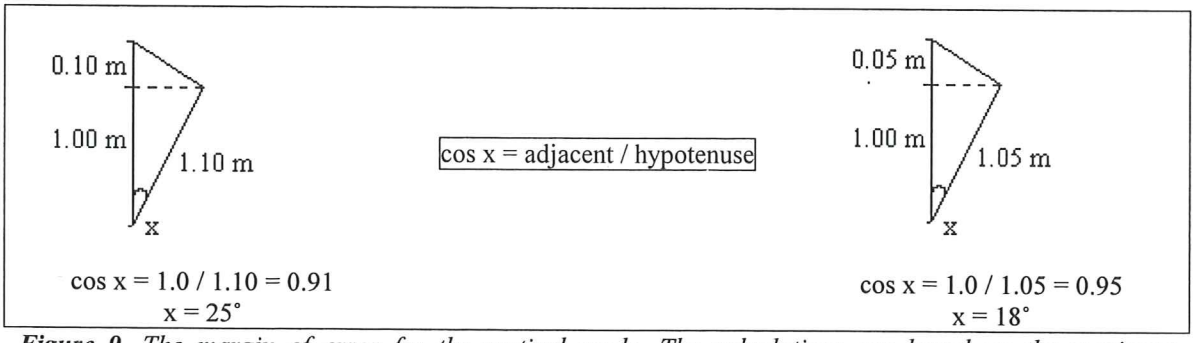

Figure 9. *The margin of error for the vertical angle. The calculations are based on the maximum differences in height for the cords (left – 30-m cord, right – 15-m cord) to keep the accuracy below 0.2°.*

To keep each gradient measurement within these errors, the poles were checked to be vertical with the angle indicator and the height of the cord was measured at the two poles. The poles never exceeded an inclination of 5°. A one meter long stick was placed on the ground next to the pole as a reference level to eliminate the effects of small variations in the topography. Finally, the aspect was measured with a SILVA compass in the direction of the cord. During the entire field collection the gradient was measured by one person, and the aspect by another person to avoid differences in the readings of the instruments.

5.2 Data analysis

Forest change, waterflow and precipitation data were analyzed to investigate if waterflow has been affected by changes in forest cover. Finally, DEMs and DTMs were statistically analyzed and evaluated.

5.2.1 Analysis of forest change, waterflow and precipitation

5.2.1.1 Forest changes 1984, 1990 and 1992

The classified and digitized vegetation maps and forest damage maps from 1984, 1990 and 1992 were used for a land cover change study. A bitmap of the seven catchments in the national park was digitized to a vector layer (Figure 10). The layer was rasterized and then used to extract the different catchments, area by area, in the six maps. A visual interpretation was performed of these maps and the other digital layers. To avoid the areas that for instance are classified as forest in 1984 but null-classified in the image from 1990 or 1992, due to deforestation and classification errors, they had to be removed with a mask. The mask was produced by overlaying the three images from 1984, 1990 and 1992 and hence the new layer consisted only of pixels that were classified. The mask was then overlaid with each forest damage map to create three new layers. Cross-tabulations for the new layers and the vegetation maps of 1984, 1990 and 1992 were calculated to yield land cover changes in the different catchments.

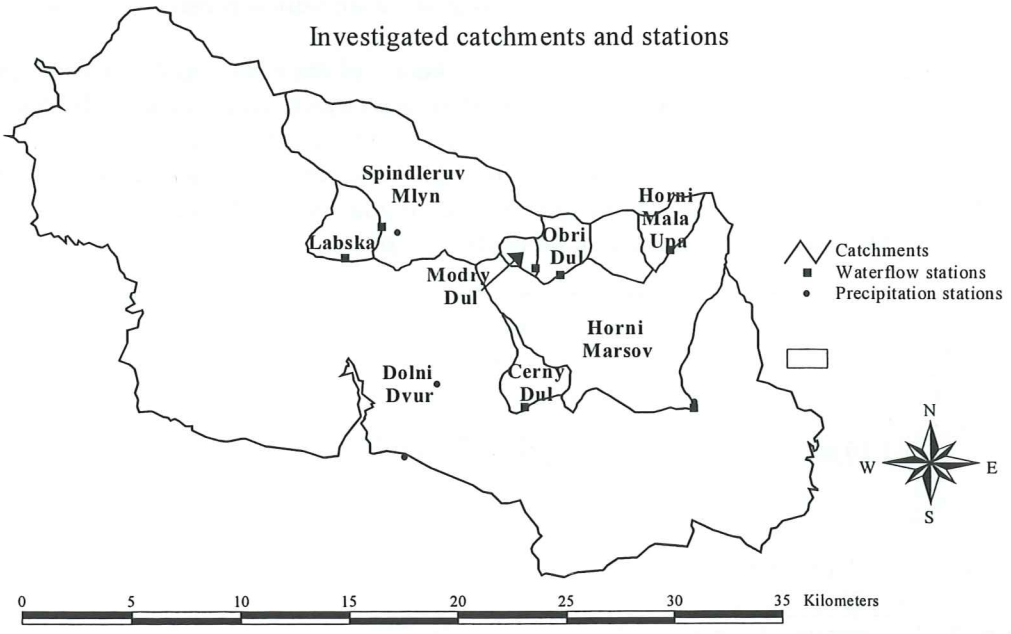

Figure 10. *The investigated catchments in the national park. The seven waterflow stations and the three precipitation stations (Spindleruv Mlyn, Dolni Dvur and Horni Marsov) are also presented.*

5.2.1.2 *Waterflow and precipitation*

To compare the different catchments with each other, specific waterflow for each area was calculated by dividing waterflow with the size of the catchment (Grip & Rodhe, 1994). The data between 1989 and 1997 were chosen for the comparison since this was the only period in common for all catchments. Both yearly averages and monthly averages for the seven areas were compared, as well as a comparison between big and small catchments. The yearly average shows waterflow in time and the monthly average shows the seasonal changes in waterflow. Data for all seven catchments were then plotted with a linear regression line (e.g. Figure 16). To avoid seasonal fluctuations, a yearly average was used from January to December. Where possible, a couple of years before and after the period were included to yield longer time series. These analyses were done to get a good overview of the material.

Precipitation data for the three stations Spindleruv Mlyn, Dolni Dvur and Horni Marsov were also plotted in graphs with linear regression lines. This was performed to analyze if the amount of precipitation had changed for the whole time series as well as for the period between 1984 and 1997. The elevation of the station was also investigated. Since there was not a precipitation station present in each catchment area, which would be desirable, only one precipitation station was chosen as a reference for the whole area. The precipitation station that agreed best with the catchments regarding elevation (Spindleruv Mlyn) was then chosen for further waterflow investigations.

Data for the precipitation station Spindleruv Mlyn and for waterflow in the catchments were plotted in the same graph to clarify the relationship between them. Correlations were also calculated between the monthly average for precipitation and waterflow during the period 1982-1994 (where possible) to see if waterflow fluctuations follow the precipitation fluctuations.

5.2.1.3 *Waterflow and precipitation ratio*

To investigate if waterflow had changed in the last few years, precipitation had to be excluded as a source for an increase or decrease. By making a ratio between the specific waterflow and the average precipitation, the influence of precipitation was standardized. This means that the ratio for every month had taken the precipitation amount for the same month into consideration. The same years are used in the analysis as for the specific waterflow. Graphs of this type can be viewed in Figure 20.

The method used in the study to investigate waterflow changes does not take evapotranspiration into consideration. A model would then most certainly be needed, for which there were not enough data. Another factor of great importance is that the run-off is assumed to be constant, that is, if precipitation increases, the run-off should increase with the same proportion.

5.2.1.4 *Catchment elevations*

Elevation and topography are important to consider when investigating different changes in precipitation and waterflow. For instance, if there are differences between the catchments despite waterflow standardization, elevation can be one of the explanations. The elevation for each area was therefore extracted from the 15-meter resolution DEM to present differences between the catchments. Histograms were made to view the frequencies of different elevations in the catchments.

5.2.2 Analysis of DEMs/DTMs

5.2.2.1 Extraction of field points from a DEM/DTM

When comparing field data with the data in a DEM/DTM, the exact point location with its attribute must be extracted from the data layer. The extraction can be performed by choosing the cell value in the DEM/DTM in which the point is located. This method was used to extract elevation, gradient and aspect in both 15-m and 30-m resolution and is from hereon referred to as PICK1. To make sure the program is picking the right coordinates in the DEM/DTM, a small grid image (3x3 cells) with known cell values and a vector file with coordinates within these nine cells were created. The image file and the vector file were then run in the program to extract the values from the image.

However, points collected in field (e.g. GPS points) are seldom located in the centre of a cell in a DEM/DTM. Taking this fact into consideration, nearby cell values should be accounted for when the values are extracted from the DEM/DTM. This extraction was performed by using an inverse distance interpolation method, called PICK2. The technique estimates the value by weighting the influence of a point value, depending on the distance to the point to be calculated. The closer the cell is to the point, the more influence it will have on the value. The cells were chosen to weight the value from four directions, shown in Figure 11. Thus, the four nearest cells were used to calculate the value of the point (e.g. the height in the DEM of that pair of coordinates). A disadvantage with this method is that pixels located in the outermost row or column cannot be calculated, due to too few surrounding pixels.

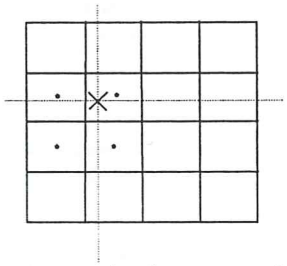

Figure 11. *The point value (cross in figure) is calculated by weighting the influence of values of the four nearest cells depending on distance. Hence, the closer the cell is to the point, the more influence it will have on the value.*

The inverse distance interpolation method can be described mathematically by:

$$g_i = \frac{\sum_{i=1}^{n}\left(\frac{x_i}{d_i^{P}}\right)}{\sum_{i=1}^{n}\left(\frac{1}{d_i^{P}}\right)} \qquad \text{Eq. 6}$$

where
g_i = estimated point value
d_i = distance between the point value and grid cell value
x_i = grid cell value
P = the power to which the distance is raised

P was set to a standard value of 2. If a data point coincided with a grid location, d = 0, the estimated value was set to the same value as of the sample point. Since PICK2 is a better method, all analyses are from hereon based on this interpolation method.

5.2.2.2 Descriptive statistics

To evaluate the GPS receiver and to investigate the difference between the DEM/DTM and the field values, the Root Mean Square Error (RMSE) was calculated. RMSE can also be expressed as the standard deviation of the residuals:

$$RMSE = \left[\sum_{i=1}^{n} \left(z_i - z^*_i \right)^2 / n \right]^{1/2} \qquad \text{Eq. 7}$$

where
n = number of sample points
i = a sample point
z = value in DEM/DTM at the sampled point
z* = field value at the sampled point

Mean, minimum and maximum were also calculated to present the statistics of the data.

To be able to make a relevant comparison between the 30-m resolution DTMs (slope and aspect), which only consist of 45 values each, with the 15-m resolution DTMs, with 104 values each, the same 45 points had to be extracted from the latter. These layers will from hereon be referred to DEMs/DTMs with a 'b' in the end.

5.2.2.3 Intervals of DEMs/DTMs

The differences between DEM/DTM and field values were divided into intervals to present the frequency and to illustrate the differences between the 15-m and the 30-m resolution layer. The difference in elevation was divided into one-meter intervals, the difference in slope into intervals of one degree and difference in aspect into intervals of five degrees. The interval size was chosen to yield around ten intervals to form an overall picture of the data.

5.2.2.4 Statistical analysis

To be able to perform certain statistical analyses it is important that the data is normally or close to normally distributed. This was investigated with a normality test called Anderson-Darling (Shaw & Wheeler, 1994). This test generates a normal probability plot and examines whether or not the observations follow a normal distribution. However, in some cases the distribution was positively skewed. Much of this skewness can, according to Shaw & Wheeler (1994), be removed by transforming the data by the taking of logarithms. Since some of the values were zero, and hence impossible to be logged, the value of 1 was added to all the observations before transformation.

The Pearson correlation coefficient (Shaw & Wheeler, 1994) was used to investigate if different datasets had a linear relationship. The correlation coefficient was calculated between:

- field value and DEM/DTM value for elevation, slope and aspect, both 15-m and 30-m resolution. This correlation indicates how strong the relationship is between observed field value and map value.
- 15-m and 30-m resolution DEM/DTM for elevation, slope and aspect. This correlation shows how well the two resolutions coincide.
- difference in 15-m and 30-m resolution DEM/DTM for elevation, slope and aspect. This correlation indicates if small differences in both layers are located at the same places and large differences at the same places.
- difference in elevation and the actual field slope value. This correlation shows for instance if the differences in elevation are larger where the slopes are steep. Since aspect is a circular variable (0-360°), this kind of correlation can not be performed.

The Student's t-test performs a hypothesis test and determines if the averages of two samples are significantly different. The only assumption that needs to be made is that the distribution is normal or close to normal (Shaw & Wheeler, 1994). In this study, the test was used to investigate if the average of the differences (between field value and DEM/DTM value) was significantly separated from zero. This will then indicate that the difference is to great to be attributed to random variation. The hypothesis for the t-test was set to:

H_0 = no difference from zero can be indicated
H_1 = there is a significant difference between mean of dataset and zero

For n = 104, null hypothesis is rejected when $T > 1.96$. For n = 45, null hypothesis is rejected when $T > 2.02$. A two-tailed significance level of 0.05 was used. To remove the effects of levelling that arise when negative values are compensated by positive, i.e. the mean gets too close to zero, the absolute values of the differences were also used to perform t-tests. For example, a dataset that accepts H_0 might, when using the absolute values, reject H_0. This rejection implies that when eliminating the effects of levelling the mean is actually significantly different from zero.

6. Results

Forest damage and forest change have been analyzed both visually and statistically to investigate the spatial as well as the quantitative changes. Waterflow and precipitation analyses have also been performed. The first part of the chapter presents the results from these analyses and the second part presents the results from the evaluations of the DEMs/DTMs.

6.1 Forest damage, waterflow and precipitation

Results of both visual and statistical analyses of the forest changes are presented below. To simplify the interpretation and the analyses, locations and names of the seven catchments can be viewed in Figure 10. The results from the precipitation and waterflow analyses are also presented below.

6.1.1 Visual interpretation of forest changes

A visual interpretation of the three vegetation maps and the three forest damage maps from 1984, 1990 and 1992 was performed. The vegetation maps from 1984 and 1992 are presented in Figure 12. The layer from 1990 is not shown since the difference between 1990 and 1992 is relatively small. Figure 13 views the forest damage maps for the same two years. Maps of forest age, deforestation and topography were also used as a complement in the visual interpretation. Before a mask of forest damage was produced and applied to the three datasets of forest damage, the layers from 1990 and 1992 consisted of a large null class. When viewing the maps, this null class was mainly classified as clear-cuts in the vegetation maps for the same years.

In larger parts of the catchment Spindleruv Mlyn, the forest changed from healthy and lightly damaged to moderately and strongly damaged between 1984 and 1992. Clear-cuts are spread all over the catchment in elevations of 800-1150 m. Spindleruv Mlyn is also part of the larger catchment Labska. In the southwest part of Labska, where Spindleruv Mlyn is not included and the elevations are lower (around 800 m), the forest seems to be healthier, to a large extent in the classes healthy to moderate. The forests of the Cerny Dul catchment are mainly old (around 100 years) and healthy throughout the period. However, in relation to its area (7 km^2) a large portion, stretching from north to east at about 900-m elevation, has been cut down. This clear-cutting was, according to the deforestation map, performed mainly after 1986.

The catchments Modry Dul, Obri Dul and Horni Mala Upa are part of the larger catchment Horni Marsov. One third of the catchment Modry Dul is covered with alpine grasslands and mountain pine and it has an average elevation between 1000-1300 m. There is hardly any change in forest damage and almost no clear-cuts are present. Obri Dul is mainly covered with forests older than 100 years, which in general has changed from healthy and lightly damaged to moderately and strongly damaged between 1984 and 1992. The forest is situated in the eastern and higher part (around 1000 m) of the catchment. Horni Mala Upa consists to 50% of young forest (< 20 years) and clear-cuts. The other part consists of older forests, which are relatively damaged (moderate to strong). The clear-cuts are spread over the entire area, but they are more concentrated in the northern part at higher elevations (between 900 m and 1150 m). Horni Marsov has a lot of clear-cuts in the eastern part along the water divide. In the middle lower part the forest is healthy but at higher elevations (1000-1100 m) the forest is moderately to very strongly damaged.

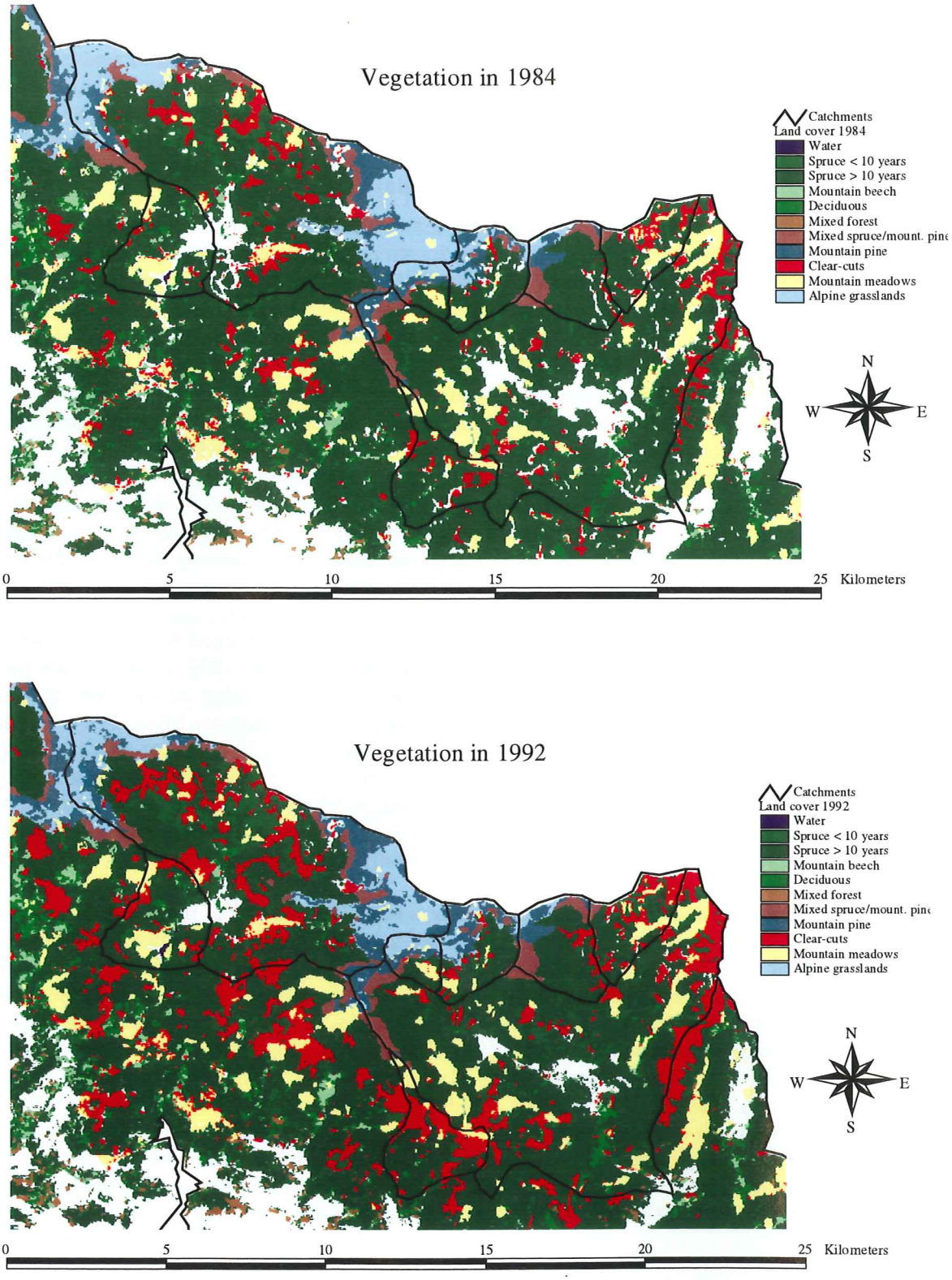

Figure 12. *Vegetation cover in 1984 (upper) and 1992 (lower). The maps are based on layers collected at KRNAP.*

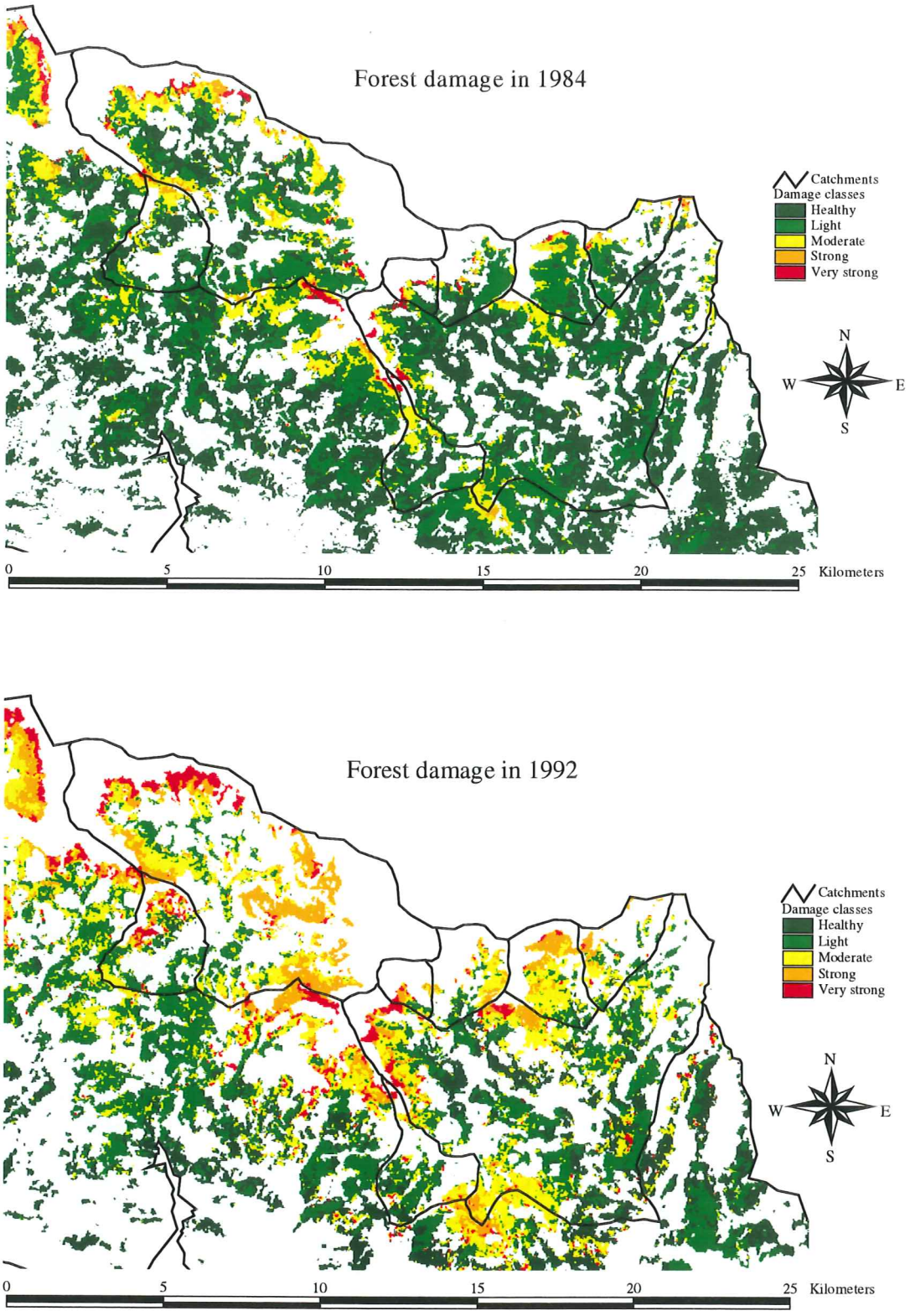

Figure 13. *Forest damage in 1984 (upper) and 1992 (lower).*

6.1.2 *Digital analysis of forest changes*

The frequency of clear-cuts for the three vegetation maps from 1984, 1990 and 1992 is presented in Figure 14. In general, there has been an increase in clear-cuts in all catchments from 1984 to 1992. The figure shows that the two smaller catchments Cerny Dul and Horni Mala Upa, which are located at lower elevations, have a dramatic increase in clear-cut frequency (23% and 10%, respectively) from 1984 to 1992. On the other hand, Modry Dul and Obri Dul, which are also small catchments but are located higher up in the system, have relatively small frequencies of clear-cuts throughout the period. The increase is only 1% and 4% respectively. The three large catchments Spindleruv Mlyn, Labska and Horni Marsov have almost the same change from 1984 to 1992, i.e. an increase in clear-cuts of 5%.

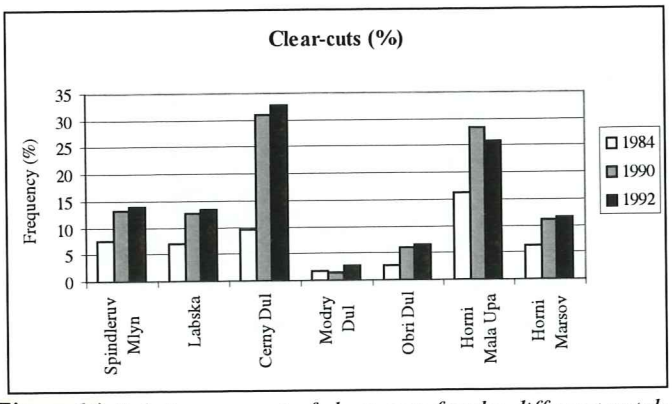

Figure 14. *Relative amount of clear-cuts for the different catchments and years.*

The frequency of forest damage classes for the different catchments and years are shown in Figure 15. The results presented in the seven graphs indicate that a shift in damage classes occurred during the period 1984 to 1992. For all catchments the general forest status altered from mainly healthy and lightly damage to mostly lightly, moderately and strongly damaged forest.

The catchments Spindleruv Mlyn and Labska are very similar to each other regarding distribution in forest damage classes. Approximately 75% of the forest was in 1984 healthy to lightly damaged. In 1992 the same percentage had turned into moderately or strongly damaged. The spruce in the Cerny Dul catchment shifted from damage classes 1 and 2 in 1984 to mainly class 2 in 1990-92. The catchment Modry Dul had a more even distribution of spread over the period. Note that the healthy forest had almost diminished in 1992 in Modry Dul (from more than 20% in 1984), whereas the strongly damaged spruce had increased almost seven times to 33% in 1992.

The forest damage changes in Obri Dul and Horni Mala Upa are very similar to each other. In 1984, almost 90% of the forest was classified as healthy or lightly damaged, whereas no more than 10% was in the classes moderate to very strong damage. In 1992, the forest in these areas had deteriorated to the extent that it could be classified as mainly moderately to strongly damaged. These two damage classes had a total increase of 65%, which is almost six times higher than in 1984. Almost the entire spruce forest of the catchment Horni Marsov was classified as healthy or lightly damaged in 1984. This percentage decreased to 55% in 1992, whereas the moderate damage class increased approximately three times over the period.

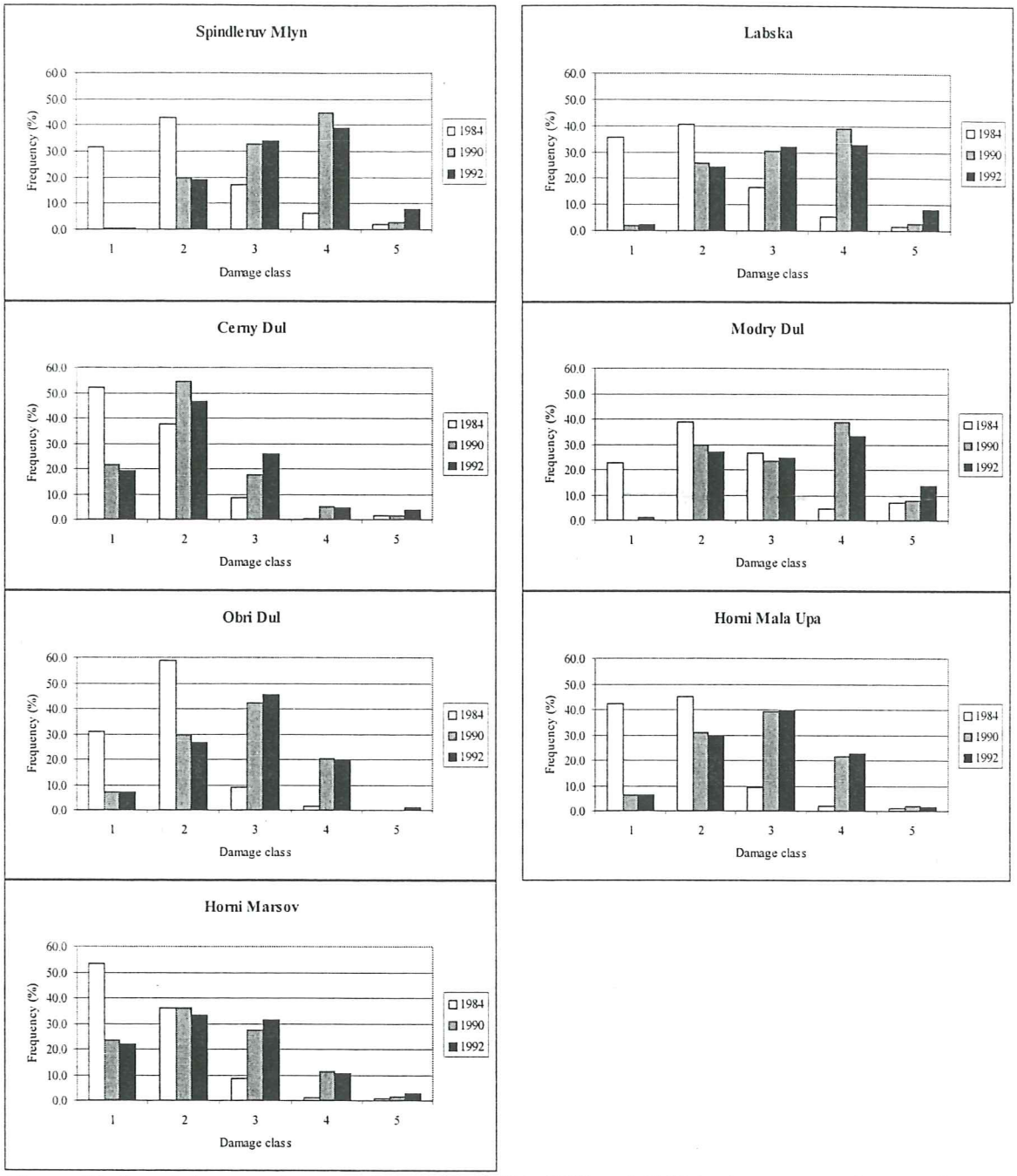

Figure 15. *Forest damage changes for the years 1984, 1990 and 1992 in the seven catchments. Damage classes: 1 = healthy, 2 =light, 3 = moderate, 4 = strong and 5 = very strong.*

6.1.3 Waterflow and precipitation

Graphs presented in Figure 16 show specific waterflow over time and a linear regression line that indicates whether or not there is a trend in the series. As shown, there are positive trends in specific waterflow for the catchments Spindleruv Mlyn and Horni Mala Upa. The catchments Modry Dul and Obri Dul, on the other hand, show very weak negative trends whereas Labska, Cerny Dul and Horni Marsov show no trend at all. Cerny Dul has a large waterflow peak around 1986, which is also present but not as distinct in Modry Dul during the same period.

Unfortunately, the other catchments lack data for this period, so it is impossible to determine whether the entire area is affected or if it could be a local phenomenon. The graphs indicate that all catchments have an increased waterflow from approximately 1993 to 1995, which is clearly shown in Cerny Dul but also in Obri Dul and Horni Mala Upa.

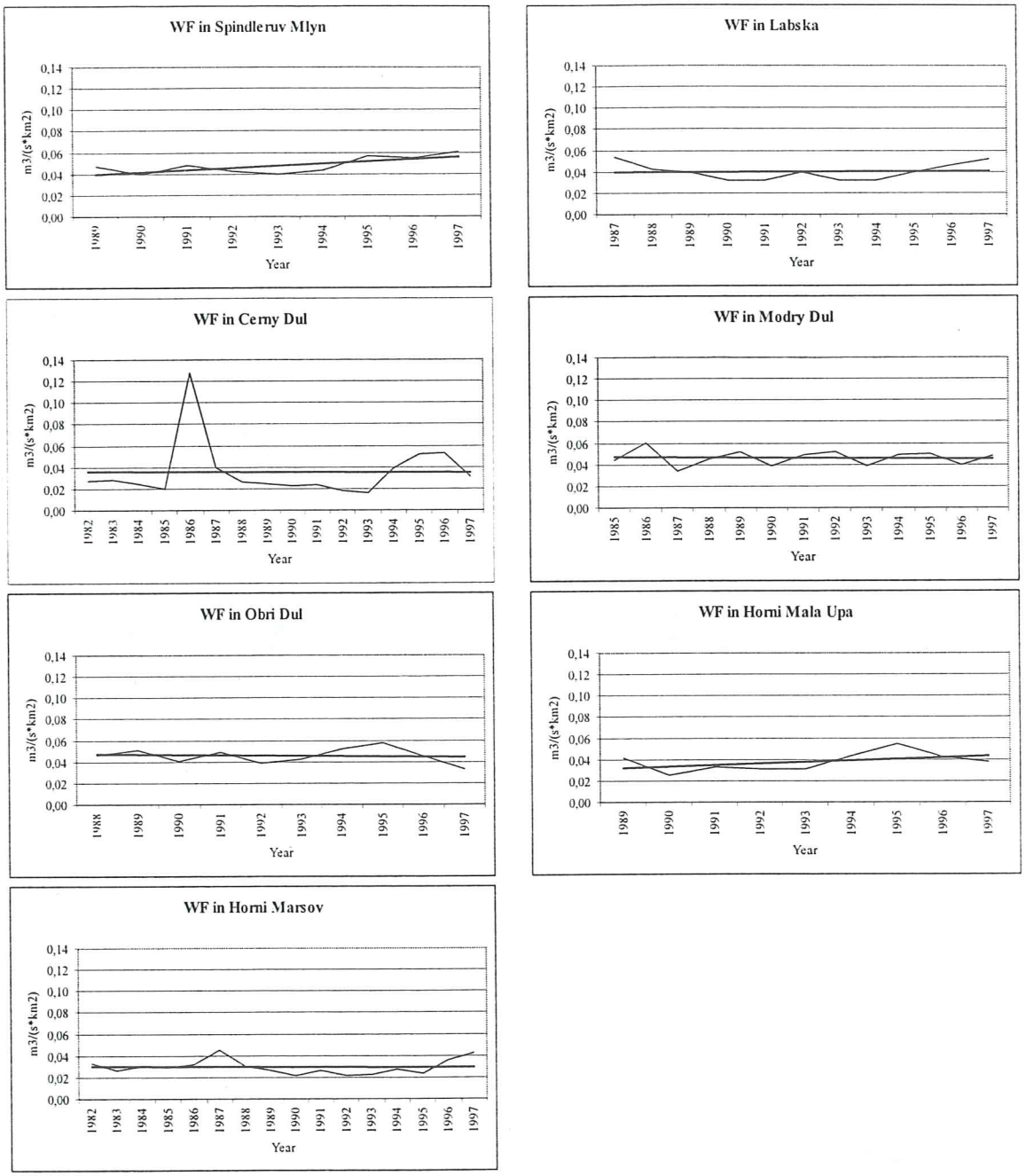

Figure 16. *Analysis of specific waterflow over time in the seven catchments. Linear regression lines have been added to indicate if there is a trend in data. WF is the abbreviation of waterflow. Note the different time scales.*

When specific waterflow for all areas are compared it is noticed that data differ from area to area, except for the period around 1995 when all areas have an increased specific waterflow, as mentioned above. This increase is clearly shown in Figure 17, which is a comparison of the catchments (Figure 17). The data for the three larger catchments are plotted in the left graph and the four smaller in the right graph. If data for all seven catchments were plotted in one graph it would be difficult to discern the series.

Horni Marsov has lower values throughout the entire series than the other two larger catchments (left). For the smaller catchments, Cerny Dul and Horni Mala Upa have the lowest values (right), whereas Obri Dul and Modry Dul are fairly similar to each other regarding waterflow. All catchments except Horni Marsov have a specific waterflow value of 0.05-0.06 $m^3/(s * km^2)$ in 1995, irrespective of earlier yearly averages. The figure also illustrates that Horni Marsov reaches a peak just above 0.04 $m^3/(s * km^2)$ in that same year.

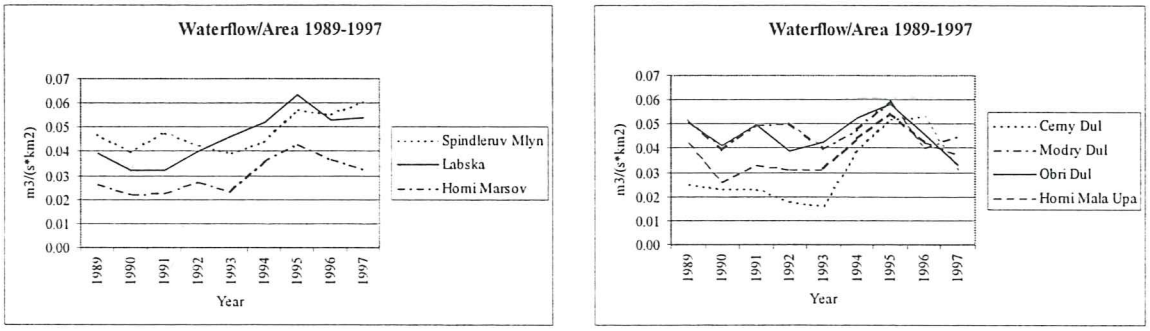

Figure 17. *Specific waterflow of yearly averages for the seven catchments. Large catchments left, smaller catchments right.*

When comparing monthly averages (Figure 18), data for the three larger catchments are plotted in the left graph and the four smaller in the right graph for the same reason as above. Spindleruv Mlyn and Labska are very similar (left). Horni Marsov has lower values throughout the entire year although it seems to have the same pattern. As for the smaller catchments (right), the differences are largest during summer months when the waterflow is high. The large catchments have high waterflow frequencies during both June and July, whereas the smaller catchments have a more concentrated peak in either June or July.

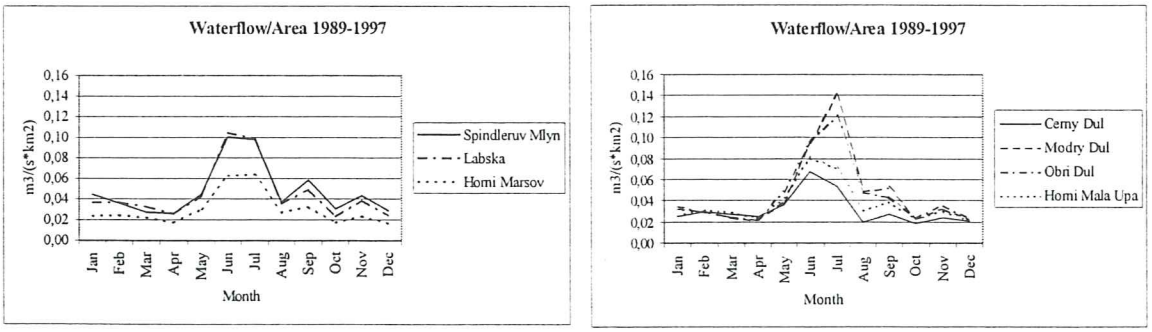

Figure 18. *Specific waterflow of monthly averages for the seven catchments. Large catchments left, small catchments right.*

The analysis of precipitation, given in Figure 19, indicates that the three stations located in the national park - Spindleruv Mlyn, Dolni Dvur and Horni Marsov - have positive trends for the period 1982-1997 (Spindleruv Mlyn 1982-1994). However, the precipitation station Spindleruv Mlyn is situated at a height of 852 m, which agrees better with the heights of the different catchments (stations located between 570 and 1026 m) compared to an elevation of approximately 600 m for the other two precipitation stations.

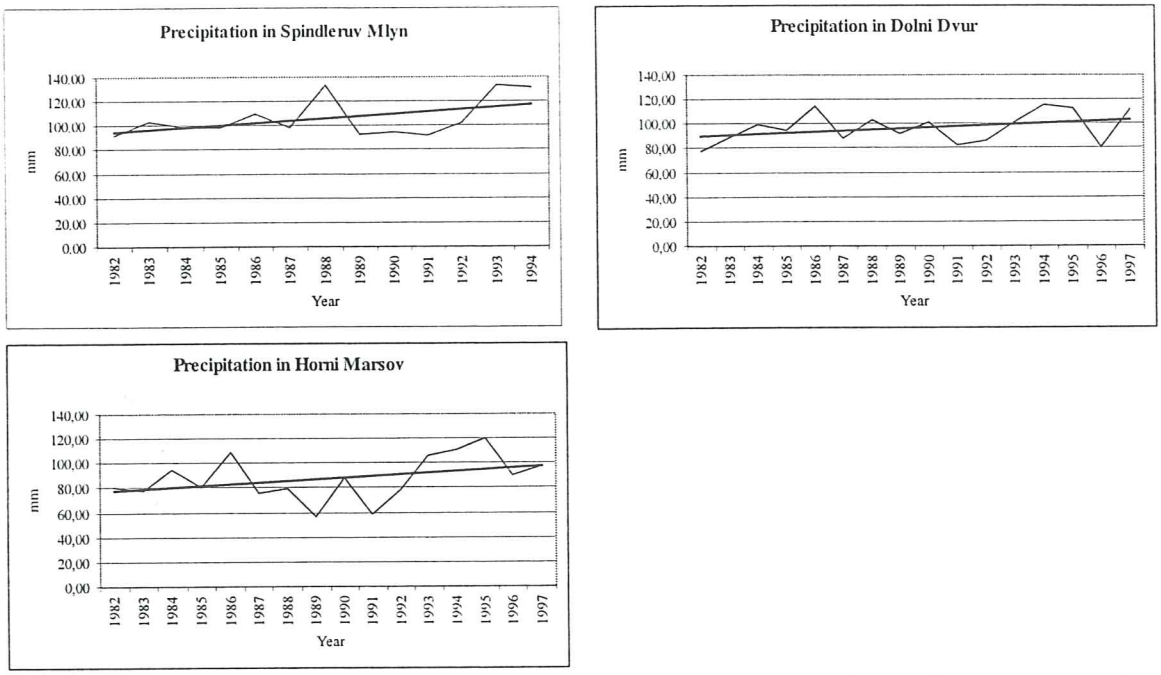

Figure 19. *Precipitation over time with linear regression lines for the period 1982-1997 (Spindleruv Mlyn 1982-1994) for the three stations located inside the national park.*

The precipitation data measured in the station Spindleruv Mlyn and the waterflow data of yearly averages were plotted in the same graph to determine how well they coincided with each other. In Appendix 1 the graphs show that the variables do not agree very well. This result is also strengthened in that correlations between monthly averages of precipitation and waterflow are weak for all catchments ($r < 0.25$, 95% significance level).

6.1.4 Waterflow and precipitation ratio

To standardize the influence of precipitation on specific waterflow, and to detect the actual periodical waterflow change, ratios between the two variables (specific waterflow/precipitation) were calculated. Since specific waterflow was used, the size of the catchment also had been standardized.

The results show in Figure 20 that all stations yielded a negative trend. The catchments Spindleruv Mlyn and Horni Mala Upa had the largest change since they, before rationing, were the only catchments with positive trends, as given in Figure 16. However, the general waterflow change from 1982 (where possible) to 1994 is approximately the same as when compared to graphs of specific waterflow (Figure 16). Peaks are located in the same years in both analyses. For example, the peak in Cerny Dul and Modry Dul in 1986 is not affected by the precipitation variation.

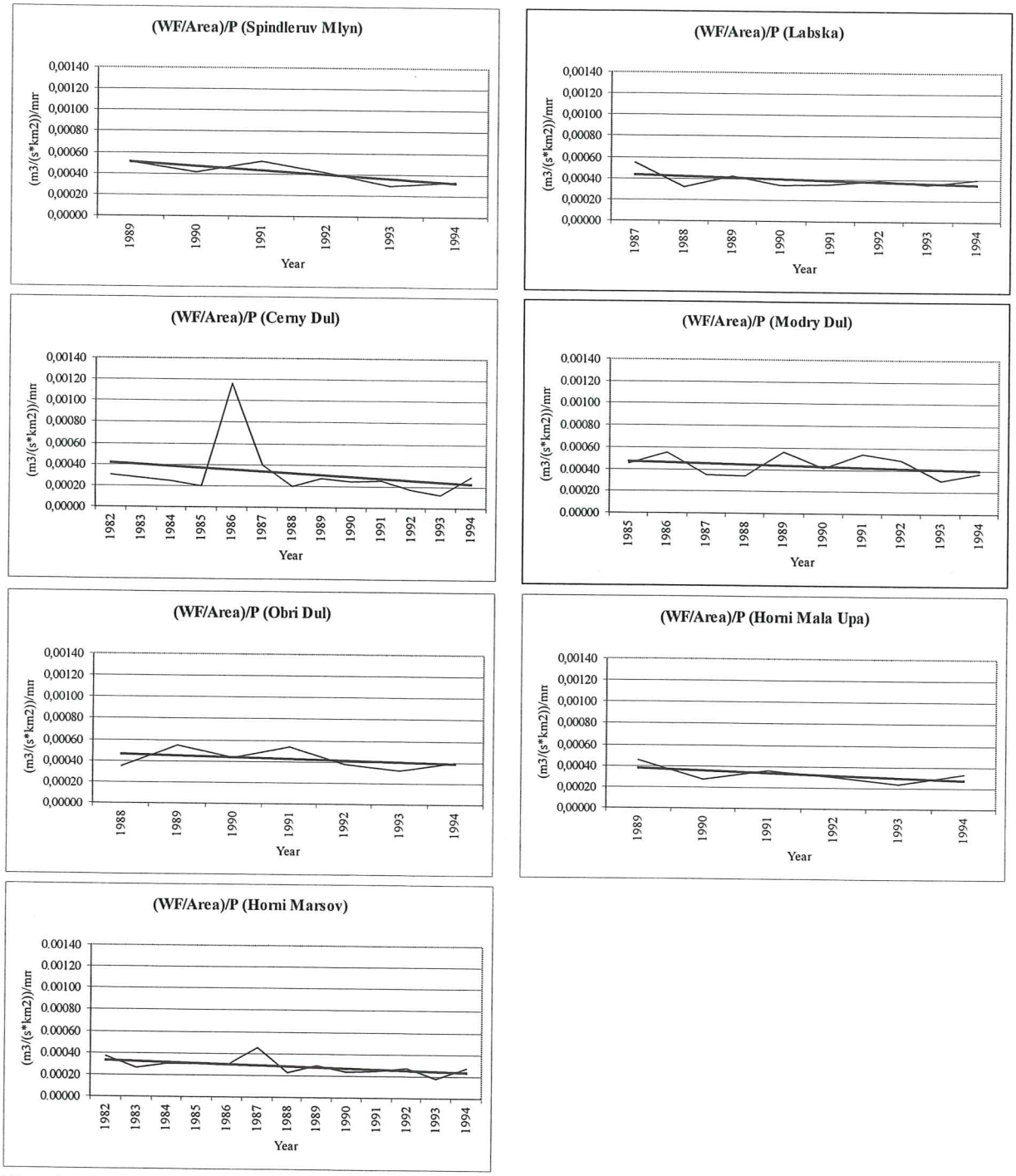

Figure 20. *Analysis of the ratio between specific waterflow and precipitation for the seven catchments. Note the different time scales.*

6.1.5 Catchment elevations

Elevations of the catchments were extracted from the topographic map (Figure 21) to yield the general topography of the areas. This data was needed for comparison of the catchments regarding waterflow. The elevations for the different catchments vary between 557 m and 1604 m.

Appendix 2 shows the histograms of the elevation for each area. Note the regular peaks with large frequencies in the graphs. These peaks are the isolines, which are over represented from the rasterization of the contour lines.

The larger areas are more equally spread regarding elevation compared to the smaller areas. Spindleruv Mlyn and Labska have the highest frequencies approximately between 800 m and 1500 m while Horni Marsov lies between 650 m and 1350 m. For the smaller areas, Cerny Dul and Horni Mala Upa have the largest frequencies between 900 m and 1200 m, Modry Dul between 1000 m and 1500 m and Obri Dul between 900 m and 1400 m.

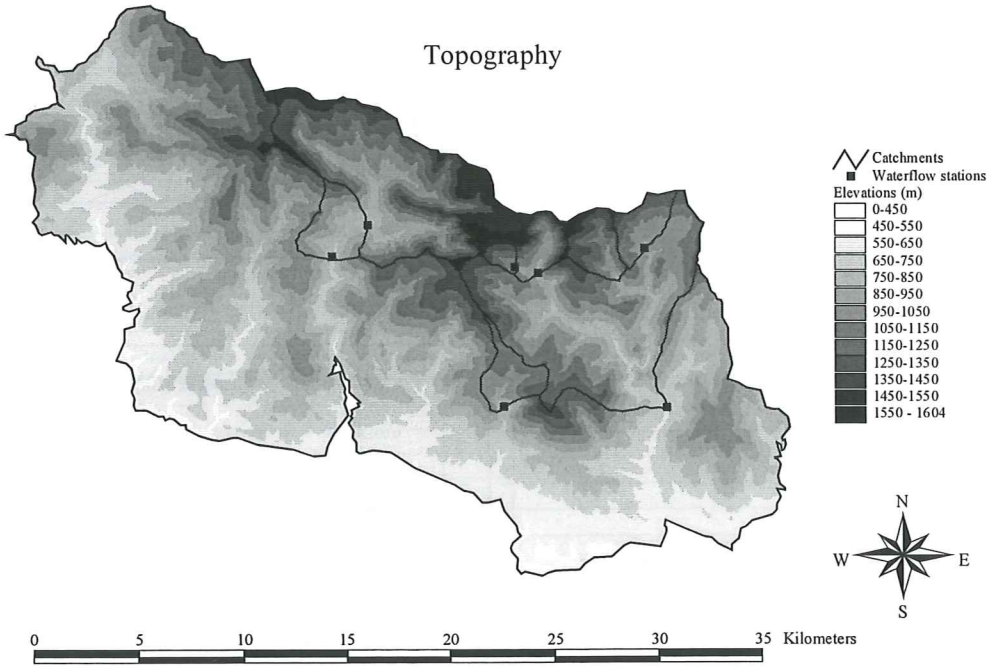

Figure 21. *Digital Elevation Model with catchments and waterflow stations in the national park. The map is based on digital layers collected at KRNAP.*

6.2 Evaluation of GPS receiver

The differences between the five geodetic points and the GPS receiver vary from –0.43 to 0.1 m in west-east (x) direction, 0.38 to 1.44 m in south-north (y) direction and –1.19 to 0.92 m in elevation (z). Table 7 shows that the lowest RMSE value in all three directions is yielded when receiving 900 positions, despite the fact that it has the highest PDOP.

Table 7. Average PDOP, mean of the differences and RMSE values in x, y and z direction.

	PDOP	Mean X (m)	RMSE X (m)	Mean Y (m)	RMSE Y (m)	Mean Z (m)	RMSE Z (m)
All positions (n = 9)	3.79	-0.20	0.24	0.84	0.90	0.07	0.67
900 positions (n = 5)	4.22	-0.18	0.18	0.80	0.80	0.29	0.65
450 positions (n = 4)	3.25	-0.21	0.29	0.94	1.02	-0.21	0.70

6.3 Evaluation of DEMs/DTMs

6.3.1 Differences between two extraction methods

Statistics for the differences between PICK1, which is a nearest neighbour operation, and PICK2, which uses an inverse distance interpolation when extracting pixels, are viewed in Table 8. Slope15b and Asp15b (Asp = Aspect) represent the 45 values with the same coordinates as for Slope30 and Aspect30. 15 and 30 stands for 15-m and 30-m resolution, respectively.

The 15-m resolution DEM (DEM15) is only marginally better (closer to zero) when using PICK2 instead of PICK1, regarding all statistics. However, when comparing the two methods for DEM30, PICK2 is obviously the better one. The maximum value is remarkably lower and the RMSE has decreased with a full meter. There are hardly any differences between PICK1 and PICK2 in either slope or aspect DTMs.

6.3.2 Descriptive statistics of 15-m and 30-m resolution DEMs/DTMs

Statistics for the difference between field value and the DEM/DTM, when using PICK2, are also presented in Table 8. For the DEMs, the 15-m resolution DEM has generally lower values than the 30-m resolution DEM. Regarding slope, the 30-m resolution DTM has lower values than both Slope15 and Slope15b with the exception of the mean value for Slope15. Slope15b is also lower than Slope15 in all cases except for the mean value. Asp15b is lower than both Asp30 and Asp15, with the latter one as the worst DTM.

Table 8. Minimum, maximum, standard deviation, mean and RMSE calculated for the difference between the field value and the DEM/DTM, 15 and 30-m resolution. PICK1 uses a nearest neighbour operation to extract pixels, whereas PICK2 uses inverse distance interpolation. Asp is the abbreviation for aspect. Slope15b and Asp15b are the 45 values with the same coordinates as for Slope30 and Asp30, respectively.

		DEM15 n = 104 (m)	DEM30 n = 104 (m)	Slope15 n = 104 (°)	Slope30 N = 45 (°)	Asp15 n = 104 (°)	Asp30 N = 45 (°)	Slope15b n = 45 (°)	Asp15b n = 45 (°)
PICK 1	Min	-8.5	-10.9	-11.5	-4.3	-65.5	-43.3	-7.4	-43.0
	Max	8.7	17.6	11.6	7.2	30.8	36.0	11.6	30.8
	STD	3.0	4.2	3.6	2.4	16.9	18.1	3.1	15.3
	Mean	0.4	0.4	0.2	0.8	-10.7	-7.1	0.9	-7.1
	RMSE	3.0	4.2	3.6	2.5	20.0	19.3	3.3	16.7
PICK 2	Min	-8.4	-10.3	-11.5	-4.1	-64.9	-44.6	-7.2	-42.3
	Max	8.3	11.9	12.8	8.0	51.4	36.2	11.8	31.2
	STD	2.8	3.2	3.6	2.4	17.3	18.2	3.1	14.8
	Mean	0.3	0.3	0.4	0.8	-9.5	-6.8	0.9	-6.7
	RMSE	2.8	3.2	3.6	2.5	19.6	19.3	3.2	16.1

6.3.3 Intervals of DEMs/DTMs

The differences between field values and DEM/DTM values were divided into intervals to illustrate the distinction between the 15-m and the 30-m resolution layer. Figure 22 presents the interval frequency for DEM15 and DEM30. DEM15 has 36% of its values within one meter and 93% within five meters, whereas DEM30 has 30% in the first interval and 89% within five meters. As shown in the figure, 100% of the values are within 10 meters for DEM15 and within 12 m for DEM30.

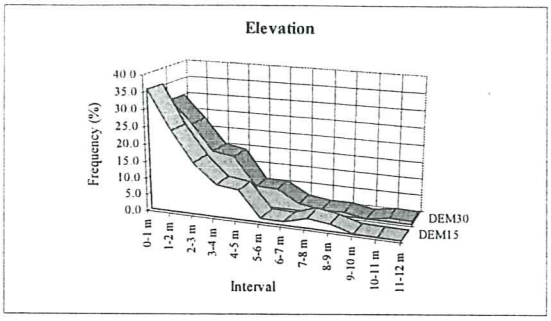

Figure 22. *Frequency distribution of 15-m and 30-m resolution DEMs.*

In contrast to the elevation layers, the 30-m Slope DTM (Figure 22, left) has the highest accuracy of the three, although the differences are small (around 5% within five meters). DTM15 and DTM15b have the same general frequency distribution with 100% of the values within 12 degrees, compared to 9 degrees for DTM30. However, DTM15b has a more concentrated distribution than DTM15 in the first four intervals.

When comparing Aspect DTMs (Figure 23, right), DTM15b has the highest accuracy. It has 87% of its values within the first five intervals (25 degrees), whereas DTM15 and DTM30 have 79%. All the values of DTM15b and DTM30 are distributed within 45 degrees (nine intervals) whereas 100% of the DTM15 values are within 65 degrees.

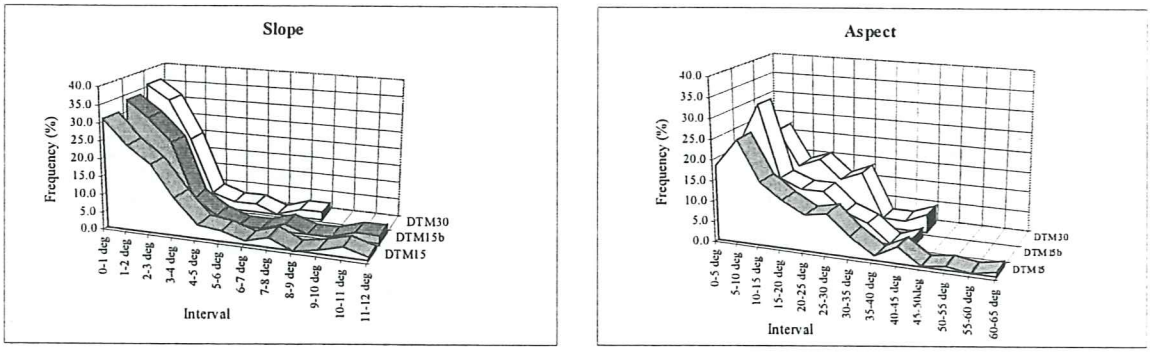

Figure 23. *Frequency distribution of 15- and 30-m resolution DTMs (slope to the left and aspect to the right). DTM15b – the 45 values in DTM15 with the same coordinates as for DTM30.*

6.3.4 Statistical analysis

The normality test Anderson-Darling indicated that all datasets (DEMs/DTMs with 15-m and 30-m resolution) were normally distributed. However, the absolute values were tested as well. Since these values were positively skewed, they were log transformed, which resulted in normally distributed data.

The Pearson correlation coefficient, r, and the coefficient of determination, r^2, were calculated for different datasets. The calculations between field value and DEM/DTM (Table 9) yielded correlation coefficients and coefficients of determination of 1.00 for elevation in both 15-m and 30-m resolution. The slope and aspect layers yielded correlation coefficients between 0.83 and 0.98 and coefficients of determination between 0.68 and 0.98, Slope and Aspect respectively. The calculations between the 15-m and the 30-m resolution gave correlation coefficients between 0.93 and 1.00 and coefficients of determination between 0.80 and 1.00, Slope and Elevation

respectively. The coefficients were calculated for the differences in the DEMs/DTMs between 15-m and 30-m resolution. The correlation coefficients varied between 0.73 and 0.81 and the coefficients of determination between 0.53 and 0.66, Slope and Elevation respectively.

Table 9. Correlation coefficients and coefficients of determination for different variables with a confidence interval of 99%. Elv = elevation, Slp = slope and Asp = aspect. 15 = 15-m resolution, 30 = 30-m resolution. n = 104, * n = 45.

Variables	Correlation Coefficient (r)	Coefficient of Determination (r^2)
ElvField-Elv15DEM	1.00	1.00
ElvField-Elv30DEM	1.00	1.00
Slp15Field-Slp15DTM	0.83	0.68
Slp30Field-Slp30DTM*	0.90	0.80
Asp15Field-Asp15DTM	0.89	0.80
Asp30Field-Asp30DTM*	0.98	0.95
Elv15DEM-Elv30DEM	1.00	1.00
Slp15DEM-Slp30DTM*	0.93	0.86
Asp15DEM-Asp30DTM*	0.99	0.98
DiffElv15-DiffElv30	0.81	0.66
DiffSlp15-DiffSlp30*	0.73	0.53
DiffAsp15-DiffAsp30*	0.74	0.55

The coefficients were also calculated between the difference in elevation and the actual field slope values. The correlation coefficient was -0.125 for the 15-m resolution layer and 0.017 for the 30-m resolution layer, indicating that there are no significant relationships between these two datasets.

Student's t-test was used to investigate if the mean of the differences between DEM/DTM and field value was significantly different from zero (if H_0 = rejected). The results are viewed in Table 10 where a two-tailed significance level of 0.05 was used. There were four layers that yielded an accepted null hypothesis: 15-m resolution DEM, 30-m resolution DEM, 15-m resolution DTM of slope and finally the 15-m resolution DTM of slope with only the 45 values that are the same as for the 30-m resolution DTM. Because the differences were both negative and positive, the average value was affected. Therefore the differences were logged and the t-test recalculated, resulting in rejected null hypotheses for all four layers.

Table 10. For n = 104, null hypothesis is rejected when t > 1.96. For n = 45 (*), null hypothesis is rejected when t > 2.02. A two-tailed significance level of 0.05 is used (Shaw & Wheeler, 1994).

Variable	N	Mean (m)	STD (m)	SE Mean (m)	t	Null hypothesis (H_0)
Elv15	104	0.4	3.0	0.3	1.28	*Accepted*
LogElv15	104	0.5	0.2	0.0	19.29	Rejected
Elv30	104	0.4	4.2	0.4	0.99	*Accepted*
LogElv30	104	0.5	0.3	0.0	20.64	Rejected
Slp15	104	-0.2	3.6	0.4	-0.68	*Accepted*
LogSlp15	104	0.5	0.3	0.0	18.03	Rejected
Asp15	104	10.7	16.9	1.7	6.45	Rejected
Slp30*	45	-0.8	2.4	0.4	-2.33	Rejected
Asp30*	45	7.1	18.2	2.7	2.63	Rejected
Slp15*	45	-0.9	3.1	0.5	-1.94	*Accepted*
LogSlp15*	45	0.2	0.4	0.1	2.58	Rejected
Asp15*	45	7.1	15.3	2.3	3.11	Rejected

7. Discussion

7.1 Forest changes and waterflow

In all catchments there has been an obvious increase in clear-cuts and forest damage (Figures 12 to 15) from 1984 to 1992. The three vegetation maps from 1984, 1990 and 1992 were evaluated by the producer of the layers. The remaining maps were not evaluated, but during the visual interpretation it was clear that they corresponded well to the evaluated maps. For instance, clear-cuts in the vegetation maps were located at the same place in the deforestation map, and also where forest was classified as younger than ten years in the forest age map.

The forest damage is generally located in higher elevations, above 1000 m, as mentioned in the results of the visual interpretation. Prerequisites for this local forest damage are the harsh climate and high precipitation. The large amount of airborne sulphur particles in the region is deposited with rain and fog (occult deposition) in higher elevations due to orographic uplift. Hence, most of the year, the higher elevations in the national park are covered with fog or clouds and are exposed to constant sulphur deposition. The phenomenon of fog and clouds in higher elevations in combination with deposition of pollution particles has been discussed by several authors (Dollard *et al.*, 1983; Nelleman and Frogner, 1994; Grossinho, 1996; Ardö *et al.*, 1997).

In the eastern part of Horni Marsov a lot of forest has been cut down despite the fact that the forest is not damaged in that area (Figure 12). This seems to be a general issue at lower elevations where forest has been removed, since these areas are easy to reach. On the other hand, it can be a part of the forest management plan where mono-cultural spruce is replaced with original mixed forest. The deciduous forest would not survive in higher elevations with harsh climate and is therefore regenerated in these lower areas. The fact that the national park is visited by several millions of people every year can also contribute to the exploitation of land. The lower regions in the national park are located in Zone III or the buffer zone (Figure 4), i.e. there are no restrictions towards clear-cutting, as long as it is performed to prevent negative influences on the park.

Regarding waterflow, Horni Marsov has lower values for both yearly and monthly averages (Figure 17 and 18), compared to the other two larger catchments. This applies for Cerny Dul and Horni Mala Upa, as well, compared to Modry Dul and Obri Dul. The areas Horni Marsov, Cerny Dul and Horni Mala Upa are all the lower elevated catchments where precipitation is lower. This implies that elevation is important to encounter when investigating waterflow. The smaller and higher elevated areas Obri Dul and Modry Dul also have larger amplitude of specific waterflow in monthly average compared to the larger areas. This is the result of a combination of quick responding time because of size, high elevations with thinner or non-existing vegetation and large amounts of snow melt in late springtime.

The national park is a mountain range with large local variations in precipitation, temperature and winds (Grossinho, 1996). This fact makes it very difficult to use one single precipitation station as a source for the whole area. With a choice of not more than three stations, the precipitation station in Spindleruv Mlyn was used for trend analyses since its height agreed better with the catchment heights. The two other stations are located at around 600 m above sea level and would probably not be representative for the catchments.

The precipitation measured in the station Spindleruv Mlyn has a positive trend (Figure 19) during the period 1982 to 1994. This trend can not be clearly viewed in the analyses of specific waterflow. However, the catchment Spindleruv Mlyn has a slightly positive trend, which can perhaps be explained by the fact that the precipitation station is located in the same area. Hence, it would have been preferable if there had been a precipitation station located in the centre or upper part of each catchment. Another solution could have been the interpolation of yearly averages, but then it would not be enough data with just the three precipitation stations that are present in the area.

When specific waterflow and precipitation are plotted in the same graph (Appendix 1), there seem to be no relationships at all. Hence, correlations between precipitation and specific waterflow are generally very weak. This can be a result of the lack of precipitation stations and the short time series. The fact that neither evapotranspiration nor different storages have been taken into consideration may have influenced the results as well. The evapotranspiration, for example, is depending on air temperature and, unfortunately, data for this parameter was lacking. A lot of the precipitation in these mountains is in the form of snow. If yearly averages from January to December are used, the stored winter precipitation in a specific year does not show in the statistics until the snow and ice has melted in late spring the year after. This can perhaps be avoided if the yearly average is calculated from October to September the following year.

When comparing graphs of specific waterflow with the ratio of waterflow and precipitation (Figure 20), all the catchments yielded negative trends. This can be the result of an increasing trend in precipitation for the same period. This increase in precipitation has probably not been large enough to be detected as increased waterflow. The forest and the vegetation can have adapted its interception capacities to the increase in precipitation and hence the overland runoff does not increase. The negative trend can also be due to the fact that the year 1995 (with a peak in waterflow) is excluded since there is no precipitation data for that year.

The method used does not take precipitation variations regarding runoff into consideration. The evapotranspiration could as well have become higher due to an increasing trend in temperature, which has not been investigated. However, the peak that has developed from 1993 to 1995 in specific waterflow for all catchments (Figures 16 and 17) can most certainly be the result of a peak in precipitation for all three stations. Horni Marsov had the highest measured precipitation in 1995 since the measurements started in 1951. Spindleruv Mlyn and Dolni Dvur almost reached their highest values as well during the period 1993 to 1995 since the beginning of the measurements.

In 1986, there is also a peak in precipitation in both stations Dolni Dvur and Horni Marsov (Figure 19). But this can not be detected in waterflow except for the catchment Cerny Dul series, which had a large peak (Figure 16). This peak can be explained not only by precipitation but also by a large change in forest cover. It can be viewed in the deforestation map that from the year 1986, 20% of the healthy forest in Cerny Dul was cut down. The area is so small that this amount of deforestation probably has a great impact on the catchment. After approximately three years the waterflow values were back at the same level as before the deforestation. According to Hornbeck *et al.* (1993), it is only the first year after clear-cutting that the waterflow is greatly affected by it. After that, lower vegetation has been established and it probably intercepts a lot of the precipitation. This can explain the large peak in waterflow, which quickly returned to the original level. The peak does not seem to be a measuring error since all values through the whole year are very much higher than for other years.

The large peak in precipitation in 1988 for the station Spindleruv Mlyn (Figure 19) can not be detected in any catchments. It seems as if this concentrated precipitation during one season was not enough to change the waterflow. Perhaps the groundwater level was low from the year before and had capacity to receive the increased precipitation. This indicates that a couple of years of intense seasonal precipitation are needed to yield a peak in waterflow.

Smaller catchments and longer time series in combination with large changes in land cover or precipitation are probably needed for the researcher to be able to detect changes in waterflow when only considering precipitation and waterflow. All variables included in the mass balance equation, i.e. runoff, evapotranspiration and different kinds of storages, are of such great importance that they can not be excluded in investigations of waterflow in shorter time periods. The best method may be to apply a hydrological model on the data, but this would be very time and data consuming. It would also have been of great help if a large and a small control catchment with no forest change during the investigated period had been present. The other catchments could then have been calibrated with these two control catchments, depending on size.

7.2 Evaluation of DEMs/DTMs

A Trimble GPS receiver with an RMSE of 0.18 m in x-direction, 0.80 m in y-direction and 0.65 m in elevation was used for the analysis of elevation, slope and aspect. These RMSEs has not been taken into consideration in the results and should therefore be regarded as a source of error. The error in x- and y-direction is not that large that it affects the result in the DEMs/DTMs, since the resolution is not lower than 15 m. In z-direction, the RMSE for the DEMs are so low (2.8 m and 3.2 m) that RMSE for the GPS can affect the results.

The angle meter INOGON90® has an accuracy of 0.2°. Theoretically it was calculated how much the poles could vary in height and inclination (Figures 8 and 9). The measurements were within these margins, but in practice it can be difficult when obstacles of different sizes may cause problems to decide what is actually the ground surface. This can cause errors in slope measuring.

The aspect was measured manually with a SILVA compass. This manual reading can cause errors when it is very hard in practice to decide the direction of a slope. Shadows, trees and other larger obstacles can also trick the eye.

The small differences between the two methods PICK1 and PICK2 (Table 8) that were used to extract points from the DEMs/DTMs, can be explained by the high resolutions. The difference may be bigger if a map with a resolution of for instance 250 m was used, since two neighbouring cells can then have larger varying values. PICK1 would just use the cell value and PICK2 would interpolate a new value given the four surrounding cells.

A comparison of 15-m resolution DEM/DTM and 30-m resolution DEM/DTM was performed. As expected, DEM15 had a lower RMSE than DEM30 since the first one has the higher resolution and the interpolation method used to produce them is the same. DEM15 had an RMSE of 2.8 m and DEM30 a value of 3.2. Slope30 and Aspect30 with RMSEs of 2.5° and 19.3°, respectively, are on the other hand slightly better than Slope15 and Aspect15 (RMSE of 3.6° and 19.6°, respectively). This result can be due to that the 30-m values were measured in areas that were less dense in vegetation. The cord would otherwise be difficult to stretch in the dense forest and the satellite signals would be too low for the GPS to receive. The more open areas yielded an easier interpretation of the main slope direction.

The field values and the different DEMs/DTMs in both resolutions are very strongly correlated. However, t-tests also imply that there is a systematic error in the differences between field values and DEMs/DTMs. The reason for this error is hard to determine. It can be caused by errors in original paper maps as well as digitization and conversion errors. It can also be a result of the methods used for interpolating isolines or when extracting points in the DEM/DTM.

8. Conclusions

There has been a large increase in forest damage and clear-cuts in all investigated catchments of the national park during the period 1984 to 1992. Forest damage is especially wide spread in higher elevations, while clear-cuts are mainly in lower or central regions of the catchments. However, no general increase in waterflow could be detected for the same period when standardizing the data. Data for the smaller catchments were more variable than for the larger catchments, which indicates that small cachments respond quicker to precipitation and land cover changes.

The result of the evaluation of digital elevation models and terrain models shows that regarding elevation, the DEM with the higher resolution had better accuracy. Slope and aspect models had just the opposite result, i.e. the 30-m resolution layers had lower RMSE. Correlations between field values and DEMs/DTMs are in general strong or very strong, indicating large agreement. However, t-tests indicate that there is a systematic error in all layers that perhaps needs further investigation.

9. References

Ahrens, C.D., 1994 (5th ed.). *Meteorology Today. An Introduction to Weather, Climate and the Environment.* West Publishing Company, USA.

Ardö, J., Lambert, N.J., Henzlík, V. & Rock, B.N., 1997. Satellite-based Estimations of Coniferous Forest Cover Changes: Krusne Hory, Czech Republic 1972-1989. *Ambio*, **26:3**, 158-166.

Bartos, M., Belochova, I., Fikejs, R., Jares, J., Pilous, V., Schuartz, O., Spatenkova, I., Strusa, J., Vasina, V. & Vavra, V., 1992. *The Krkonoše National Park.* Merkur Praha Publishing, Czech Republic.

Brewer, C.D., 1993. *The Use of Landsat Thematic Mapper and Geographic Information Systems in the Detection and Assessment of Forest Damage Occurring in the Krkonoše National Park.* Resource Administration and Management, University of New Hampshire, United Kingdom.

Cerný, J. & Paces, T., 1995. *Acidification in the Black Triangle Region.* 5th International Conference on Acidic Deposition in Göteborg, Sweden. Czech Geological Survey, Czech Republic.

Cooke, R.U. & Doornkamp, J.C., 1990 (2nd ed.). *Geomorphology in Environmental Management: a New Introduction.* Oxford Clarendon, United Kingdom.

Dollard, G.J., Unsworth, M.H. & Harvey, M.J., 1983. Pollutant transfer in upland regions by occult deposition. *Nature*, **302**, 241-243.

Dunda, K., 1991. *Frontier Parks in Czechoslovakia.* The Ministry of Environment of the Czech Republic, Czech and Slovak Federal Republic.

Gebas, J., Hrebacka, J., Jindrisek, J., Petrik, P. & Schwarz, O., 1998. *Forest management in the Krkonoše National Park.* KRNAP Administration, Czech Republic.

Grip, H. & Rodhe, A., 1994 (3rd ed.). *Vattnets väg från regn till bäck.* Hallgren & Fallgren, Sweden.

Grossinho, A.L., 1996. *Analysis of Damaged Norway Spruce Stands using Landsat Thematic Mapper and Geographic Information Systems.* London University, Great Britain.

Horn, B.K.P., 1981. Hill shading and the reflectance map. *Proceedings of the I.E.E.E.*, **69:1**, 14-47.

Hornbeck, J.W., Adams, M.B., Corbett, E.S., Verry, E.S. & Lynch, J.A., 1993. Long term impacts of forest treatments on water yield: A summary for northeastern USA. *Journal of Hydrology*, **150**, 323-344.

Hudson, N., 1981 (2nd ed.). *Soil Conservation.* Batsford Academic and Educational Ltd., United Kingdom.

Hunter, G.J. & Goodchild, M.F., 1997. Modeling the Uncertainty of Slope and Aspect Estimates Derived from Spatial Databases. *Geographical Analysis,* **29:1**, 35-49.

Jenkins, A., Peters, N.E. & Rodhe, A., 1994. Hydrology. In *Biogeochemistry of Small Catchments: A Tool for Environmental Research* (Eds. B. Moldan & J. Cerný). John Wiley & Sons, Ltd., United Kingdom.

Jones, K.H., 1998. A comparison of algorithms used to compute hill slope as a property of the DEM. *Computers & Geosciences,* **24:4**, 315-323.

Korenská, E., 1990. *Krkonoše National Park.* Krkonoše National Park Administration, Merkur, Czech Republic.

Kubíková, J., 1991. Forest dieback in Czechoslovakia. *Vegetatio*, **93**, 101-108.

Ling, K., 1995. *Air pollution and forest decline in Europe.* World Wide Fund for Nature, Switzerland.

Materna, J., unknown year. *Effects of pollution on the capacity of the vegetation to perform such functions as water retention, soil protection, wildlife habitat etc.* ECE-report, pp 242-250.

Moldan, B. & Cerný, J., 1994. Small Catchments Research. In *Biogeochemistry of Small Catchments: A Tool for Environmental Research* (Eds. B. Moldan & J. Cerný). John Wiley & Sons, Ltd., United Kingdom.

Moore, I.D., Grayson, R.B. & Ladson, A.R., 1991. Digital Terrain Modelling: A review of Hydrological, Geomorphological and Biological Applications. In *Terrain Analysis and Distributed Modelling in Hydrology* (Eds. K.J. Beven and I.D. Moore). John Wiley & Sons, England.

Nelleman, C. & Frogner, T., 1994. Spatial Patterns of Spruce Defoliation: Relation to Acid Deposition, Critical Loads and Natural Growth Conditions in Norway. *Ambio*, **23:45**, 255-259.

Pilesjö, P., 1992. *GIS and Remote Sensing for Soil Erosion Studies in Semi-arid Environments. Estimation of Soil Erosion Parameters at Different Scales.* Meddelanden från Lunds Universitets Geografiska Institutioner, Avhandlingar 114, pp 203.

Pilgrim, D.H., Cordery, I. & Baron, B.C., 1982. Effects of catchment size on runoff relationships. *Journal of Hydrology,* **58**, 205-221.

Schwarz, O., 1997. Management of Forest Ecosystems in the Krkonoše National Park, Black Triangle Region, Czech republic. In *Restoration of Forests* (Eds. R.M. Gutkowski and T. Winnicki). Kleuwer Academic Publishers, the Netherlands.

Shaw, G. & Wheeler, D., 1996 (2nd ed.). *Statistical techniques in Geographical Analysis*, David Fulton Pubishers, United Kingdom.

Skidmore. A.K., 1989. A comparison of techniques for calculating gradient and aspect from a gridded digital elevation model. *Int. J. Geographical Information Systems*, **3:4**, 323-334.

Trimble, 1995 (2nd ed.). *Mapping Systems, General Reference*. Trimble Navigation Ltd., USA.

Ulfvens, J., 1989. *Ett barr är ett liv*. Söderströms & C:o Förlags AB, Sweden.

Van der Horst, P., Vyklický, M., Skapec, L., Pauknerová, E., & Fernandes, R., 1995. Geographic Information Systems in the Management of National Parks – Data Preparation and Analysis. In J. Flousek & G.C.S. Roberts (Eds.), 1995. *Mountain National Parks and Biosphere Reserves: Monitoring and Management.* Proc. Int. Conf., September 1993, Spindleruv Mlyn, Czech Republic.

Ward, A.D. & Elliot, W.J., 1995. *Environmental Hydrology*. CRC Press, USA.

Wischmeier, W.H. & Smith, D.D., 1978. *Predicting rainfall erosion losses – a guide to conservation planning*. U.S. Department of Agriculture, Agriculture Handbook No. 537.

Young, R.A. & Mutchler, C.K., 1969. Soil Movement in Irregular Slopes. *Water Resources Research*, **5**, 1084-1089.

Appendices

Appendix I

Specific waterflow and precipitation plotted in graph for each catchment.

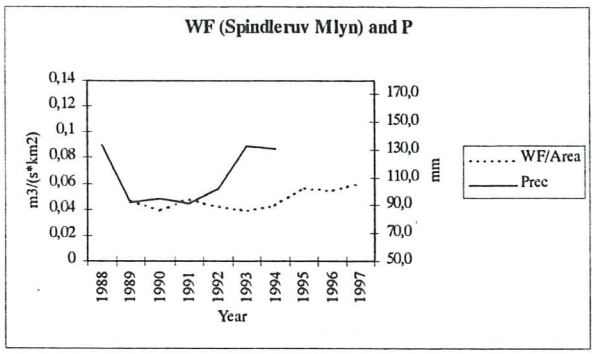

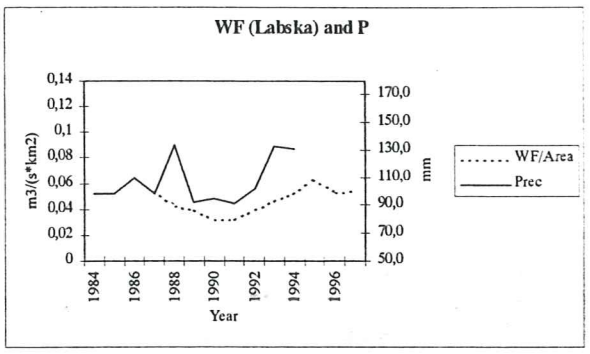

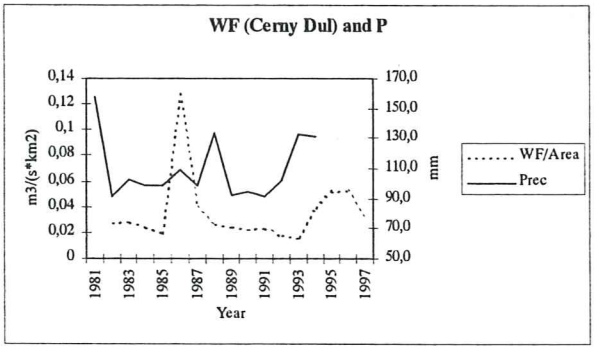

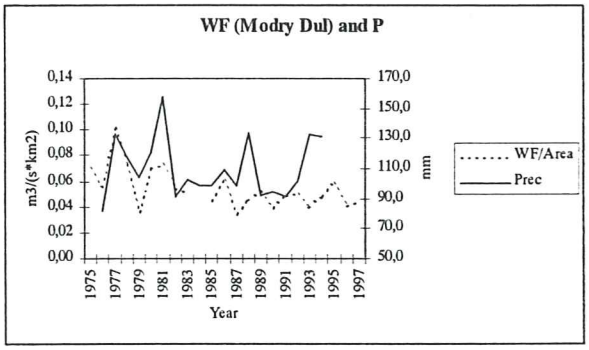

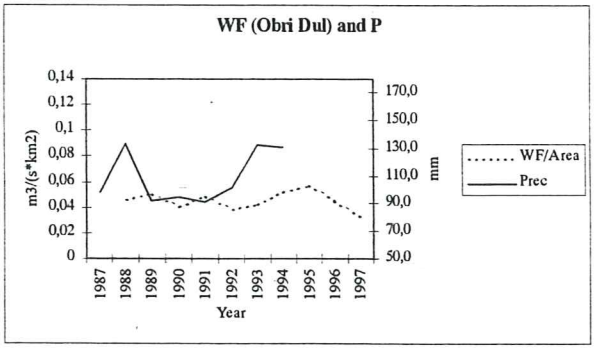

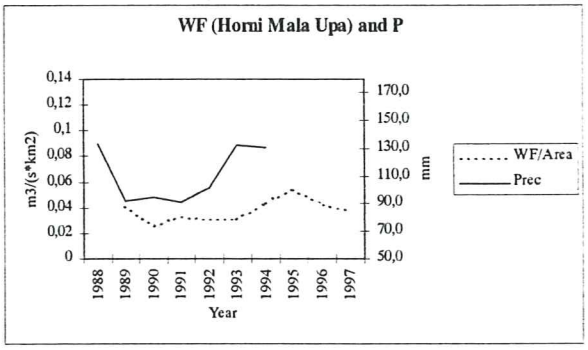

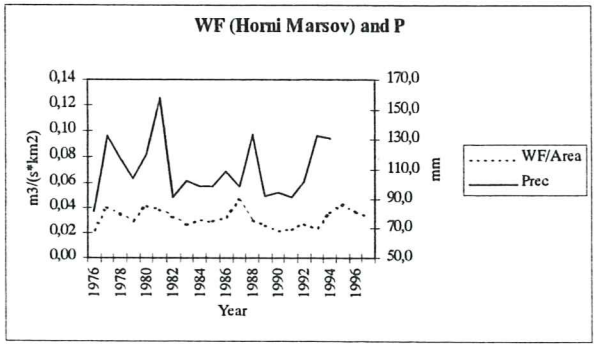

Appendix II

Extracted elevation values for each catchment.

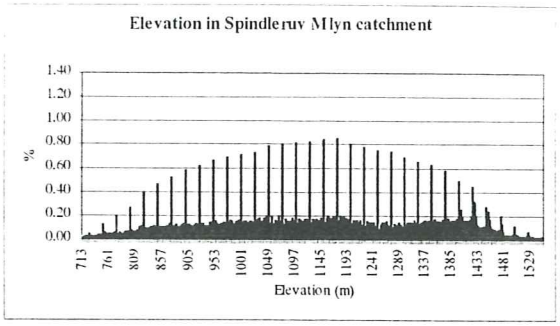

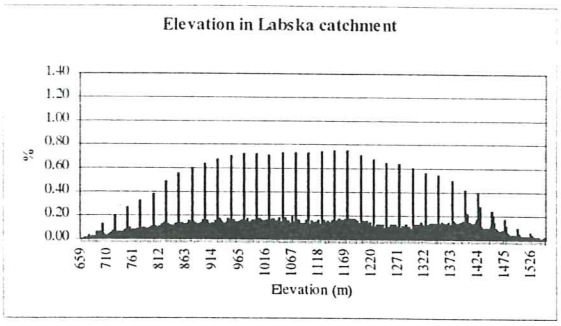

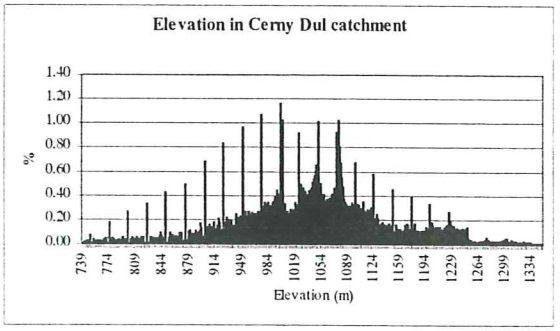

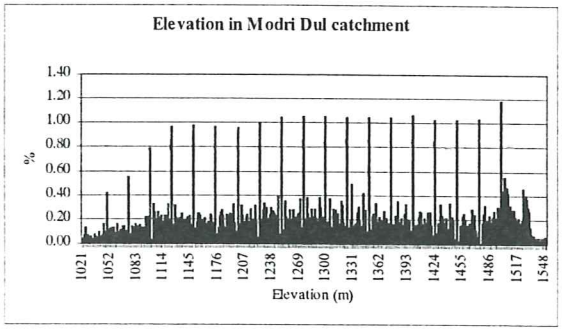

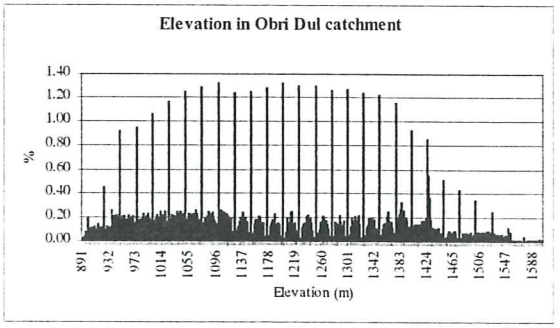

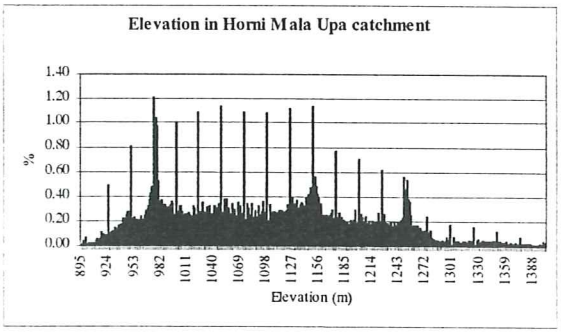

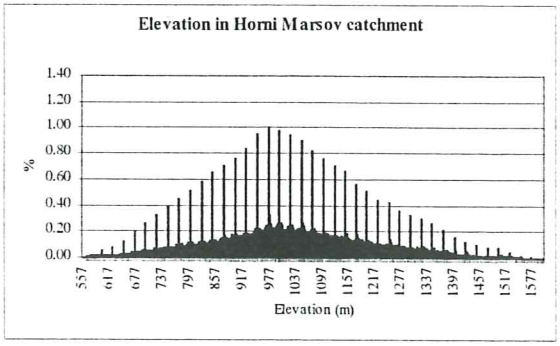

Lunds Universitets Naturgeografiska institution. Seminarieuppsatser. Uppsatserna finns tillgängliga på Naturgeografiska institutionens bibliotek, Sölvegatan 13, 223 62 LUND.

The reports are available at the Geo-Library, Department of Physical Geography, University of Lund, Sölvegatan 13, S-223 62 Lund, Sweden.

1. Pilesjö, P. (1985): Metoder för morfometrisk analys av kustområden.
2. Ahlström, K. & Bergman, A. (1986): Kartering av erosionskänsliga områden i Ringsjöbygden.
3. Huseid, A. (1986): Stormfällning och dess orsakssamband, Söderåsen, Skåne.
4. Sandstedt, P. & Wällstedt, B. (1986): Krankesjön under ytan - en naturgeografisk beskrivning.
5. Johansson, K. (1986): En lokalklimatisk temperaturstudie på Kungsmarken, öster om Lund.
6. Estgren, C. (1987): Isälvsstråket Djurfälla-Flädermo, norr om Motala.
7. Lindgren, E. & Runnström, M. (1987): En objektiv metod för att bestämma läplanteringars läverkan.
8. Hansson, R. (1987): Studie av frekvensstyrd filtringsmetod för att segmentera satellitbilder, med försök på Landsat TM-data över ett skogsområde i S. Norrland.
9. Matthiesen, N. & Snäll, M. (1988): Temperatur och himmelsexponering i gator: Resultat av mätningar i Malmö.
10A. Nilsson, S. (1988): Veberöd. En beskrivning av samhällets och bygdens utbyggnad och utveckling från början av 1800-talet till vår tid.
10B. Nillson, G., 1988: Isförhållande i södra Öresund.
11. Tunving, E. (1989): Översvämning i Murciaprovinsen, sydöstra Spanien, november 1987.
12. Glave, S. (1989): Termiska studier i Malmö med värmebilder och konventionell mätutrustning.
13. Mjölbo, Y. (1989): Landskapsförändringen - hur skall den övervakas?
14. Finnander, M-L. (1989): Vädrets betydelse för snöavsmältningen i Tarfaladalen.
15. Ardö, J. (1989): Samband mellan Landsat TM-data och skogliga beståndsdata på avdelningsnivå.
16. Mikaelsson, E. (1989): Byskeälvens dalgång inom Västerbottens län. Geomorfologisk karta, beskrivning och naturvärdesbedömning.
17. Nhilen, C. (1990): Bilavgaser i gatumiljö och deras beroende av vädret. Litteraturstudier och mätning med DOAS vid motortrafikled i Umeå.
18. Brasjö, C. (1990): Geometrisk korrektion av NOAA AVHRR-data.
19. Erlandsson, R. (1991): Vägbanetemperaturer i Lund.
20. Arheimer, B. (1991): Näringsläckage från åkermark inom Brååns dräneringsområde. Lokalisering och åtgärdsförslag.
21. Andersson, G. (1991): En studie av transversalmoräner i västra Småland.
22A. Skillius, Å., (1991): Water havesting in Bakul, Senegal.
22B. Persson, P. (1991): Satellitdata för övervakning av höstsådda rapsfält i Skåne.
23. Michelson, D. (1991): Land Use Mapping of theThat Luang - Salakham Wetland, Lao PDR, Using Landsat TM-Data.
24. Malmberg, U. (1991): En jämförelse mellan SPOT- och Landsatdata för vegetations-klassning i Småland.
25. Mossberg, M. & Pettersson, G. (1991): A Study of Infiltration Capacity in a Semiarid Environment, Mberengwa District, Zimbabwe.
26. Theander, T. (1992): Avfallsupplag i Malmöhus län. Dränering och miljöpåverkan.
27. Osaengius, S. (1992): Stranderosion vid Löderups strandbad.
28. Olsson, K. (1992): Sea Ice Dynamics in Time and Space. Based on upward looking sonar, satellite images and a time series of digital ice charts.
29. Larsson, K. (1993): Gully Erosion from Road Drainage in the Kenyan Highlands. A Study of Aerial Photo Interpreted Factors.
30. Richardson, C. (1993): Nischbildningsprocesser - en fältstudie vid Passglaciären, Kebnekaise.

31. Martinsson, L. (1994): Detection of Forest Change in Sumava Mountains, Czech Republic Using Remotely Sensed Data.
32. Klintenberg, P. (1995): The Vegetation Distribution in the Kärkevagge Valley.
33. Hese, S. (1995): Forest Damage Assessment in the Black Triangle area using Landsat TM, MSS and Forest Inventory data.
34. Josefsson, T. och Mårtensson, I. (1995). A vegetation map and a Digital Elevation Model over the Kapp Linné area, Svalbard -with analyses of the vertical and horizontal distribution of the vegetation
35. Brogaard, S och Falkenström, H. (1995). Assessing salinization, sand encroachment and expanding urban areas in the Nile Valley using Landsat MSS data.
36. Krantz, M. (1996): GIS som hjälpmedel vid växtskyddsrådgivning.
37. Lindegård, P. (1996). VINTERKLIMAT OCH VÅRBAKSLAG. Lufttemperatur och kådflödessjuka hos gran i södra Sverige.
38. Bremborg, P. (1996). Desertification mapping of Horqin Sandy Land, Inner Mongolia, by means of remote sensing.
39. Hellberg, J. (1996). Förändringsstudie av jordbrukslandskapet på Söderslätt 1938-1985.
40. Achberger, C. (1996): Quality and representability of mobile measurements for local climatological research.
41. Olsson, M. (1996): Extrema lufttryck i Europa och Skandinavien 1881-1995
42. Sundberg, D. (1997): En GIS-tillämpad studie av vattenerosion i sydsvensk jordbruksmark.
43. Liljeberg, M. (1997): Klassning och statistisk separabilitetsanalys av marktäckningsklasser i Halland, analys av multivariata data Landsat TM och ERS-1 SAR.
44. Roos, E. (1997): Temperature Variations and Landscape Heterogeneity in two Swedish Agricultural Areas. An application of mobile measurements.
45. Arvidsson, P. (1997): Regional fördelning av skogsskador i förhållande till mängd SO_2 under vegetationsperioden i norra Tjeckien.
46. Akselsson, C. (1997): Kritisk belastning av aciditet för skogsmark i norra Tjeckien.
47. Carlsson, G. (1997): Turbulens och supraglacial meandring.
48. Jönsson, C. (1998): Multitemporala vegetationsstudier i nordöstra Kenya med AVHRR NDVI
49. Kolmert, S. (1998): Evaluation of a conceptual semi-distributed hydrological model – A case study of Hörbyån.
50. Persson, A. (1998): Kartering av markanvändning med meteorologisk satellitdata för förbättring av en atmosfärisk spridningsmodell.
51. Andersson, U. och Nilsson, D. (1998): Distributed hydrological modelling in a GIS perspective – an evaluation of the MIKE SHE model.
52. Andersson, K. och Carlstedt, J. (1998): Different GIS and remote sensing techniques for detection of changes in vegetation cover - A study in the Nam Ngum and Nam Lik catchment areas in the Lao PDR.
53. Andersson, J. (1999): Användning av global satellitdata för uppskattning av spannmålsproduktion i västafrikanska Sahel.
54. Flodmark, A.E. (1999): Urban Geographic Information Systems, The City of Berkeley Pilot GIS.
55. Lyborg, J. och Thurfjell, L. (1999): Forest Damage, Waterflow and Digital Elevation Models. A Case Study of the Krkonoše National Park, Czech Republic.